

# PARAMETRIZATION AND STATISTICAL ANALYSIS OF A CARDIOVASCULAR SIMULATION MODEL

## PARAMETRIERUNG UND STATISTISCHE UNTERSUCHUNG EINES SIMULATIONSMODELLS DES HERZ-KREISLAUF-SYSTEMS

Masterarbeit

von

B. Sc. Christian Winkler

Matrikelnummer 296813

Studienrichtung:	Automatisierungstechnik
Dauer der Arbeit:	22 Wochen
Abgegeben am:	31.03.2015
Nummer:	S1791
Betreuer:	M. Sc. Jonas Gesenhues

This thesis is intended for internal use only. The copyright remains with the author and Univ.-Prof. Dr.-Ing. Abel, Institute of Automatic Control. No responsibility is taken for the content.

Die Arbeit ist nur zum internen Gebrauch bestimmt. Alle Urheberrechte liegen beim Verfasser und bei Univ.-Prof. Dr.-Ing. Abel, Lehrstuhl und Institut für Regelungstechnik. Für den Inhalt wird keine Gewähr übernommen.



I declare that this thesis has been written independently within the scope of conventional institutional supervision and no other sources than those referenced were used.

Ich versichere, diese Arbeit im Rahmen der am Institut üblichen Betreuung selbständig angefertigt und keine anderen als die angegebenen Quellen verwendet zu haben.

(Christian Winkler)

Aachen, 31.03.2015



---

# Contents

---

<b>List of Figures</b>	<b>iii</b>
<b>List of Symbols and Abbreviations</b>	<b>v</b>
<b>1 Introduction</b>	<b>1</b>
1.1 Motivation . . . . .	1
1.2 Content of this Thesis . . . . .	2
<b>2 Medical, Physical and Mathematical Background</b>	<b>5</b>
2.1 Principles of the Human Cardiovascular Physiology . . . . .	5
2.2 Data Flow and Object-Oriented Modeling . . . . .	9
2.3 Identification of Parameters in Computer Models . . . . .	10
2.3.1 Simulation . . . . .	11
2.3.2 Optimization . . . . .	11
2.4 Components and Models in the <i>HumanLib</i> . . . . .	12
2.5 Tube Element and the Equivalent Circuit Diagram . . . . .	13
2.6 Sensitivity analysis of parameters . . . . .	14
2.6.1 Local sensitivity analysis . . . . .	14
<b>3 Identification of Parameters in Models with Measured Data</b>	<b>17</b>
3.1 Preprocessing of Measured Data . . . . .	18
3.1.1 Filtering of signals LVP, AoP and AoQ with a finite impulse response filter	21
3.1.2 Transformation from LVV to LVQ and filtering . . . . .	23
3.2 Preparation of Models . . . . .	24
3.2.1 <i>HumanLib</i> elements as electrical four-terminal network . . . . .	24
3.2.2 Export to Simulink . . . . .	26
3.2.3 Inputs and Outputs of the Dymola Model . . . . .	29
3.3 Estimation Procedure and Results for Parameters . . . . .	35
3.3.1 Parameter estimation for the aorta . . . . .	36
<b>4 Statistical Study and Sensitivity Analysis</b>	<b>41</b>
4.1 Local sensitivity analysis for parameters . . . . .	42
4.1.1 Sensitivity of the aorta . . . . .	42
4.2 Sensitivity of the pulmonary circulation . . . . .	47
4.2.1 Fast sensitivity analysis with matrix representation . . . . .	48
<b>5 Discussion</b>	<b>49</b>
5.1 Measurements . . . . .	49
5.2 Equivalent circuit diagrams and the matrix representation . . . . .	50

5.3	<i>HumanLib</i> - Chances and limitations . . . . .	53
5.4	Results of parameter estimation . . . . .	55
5.5	Results of sensitivity analysis . . . . .	55
<b>6</b>	<b>Conclusion</b>	<b>59</b>
	<b>Bibliography</b>	<b>61</b>

---

# List of Figures

---

2.1	Anatomy of the heart [6] . . . . .	6
2.2	Cardiovascular system [6] . . . . .	7
2.3	Cardiac cycle for the left ventricle in the human body [6] . . . . .	8
2.4	Simulink block function . . . . .	9
2.5	Model of three tanks [1] . . . . .	9
2.6	Graphical representation of a Simulink model of the three tank system [1] . . . .	10
2.7	Identification of a process [1] . . . . .	11
2.8	<i>HumanLib</i> model based on [13] . . . . .	12
2.9	Basic objects in the <i>HumanLib</i> . . . . .	13
2.10	Tube element [4] . . . . .	13
2.11	Equivalent Circuit Diagram [4] . . . . .	13
3.1	Points of measurement [6] . . . . .	18
3.2	Measured signal LVP . . . . .	19
3.3	Unfiltered signals with noise . . . . .	19
3.4	AoP and LVP signals . . . . .	20
3.5	Unfiltered and filtered signals LVP, AoP and AoQ using a FIR filter . . . . .	22
3.6	Transformation from LVV to LVQ . . . . .	23
3.7	Dymola model with a derivative block . . . . .	26
3.8	Dymola model . . . . .	26
3.9	Diagram for the compliance with inputs $P_{in}$ and $Q_{in}$ and implemented lowpass filter . . . . .	27
3.10	Diagram for the inductance with inputs $P_{in}$ and $Q_{in}$ and implemented lowpass filter . . . . .	28
3.11	Diagram for the resistance with inputs $P_{in}$ and $Q_{in}$ . . . . .	28
3.12	Possible configurations of inputs and outputs . . . . .	29
3.13	Ursino model for the aorta . . . . .	30
3.14	Equivalent circuit diagram for the aorta . . . . .	30
3.15	Circuit diagram for the pulmonary circulation . . . . .	34
3.16	Preprocessed input and output signals . . . . .	35
3.17	$\Delta P_{aorta}$ and $\Delta Q_{aorta}$ . . . . .	36
3.18	Dymola model for aorta with configuration 6 . . . . .	36
3.19	Export model for aorta in Simulink . . . . .	37
3.20	Chosen parameters for the estimation task . . . . .	37
3.21	Setting for simulation and optimization . . . . .	38
3.22	Estimation progress . . . . .	39
3.23	Cost function and outputs . . . . .	39
3.24	Progress for parameters . . . . .	40

4.1	Extended aorta model . . . . .	42
4.2	Parameter sensitivity for the aorta . . . . .	44
4.3	Resulting progress of $i_2(t)$ . . . . .	45
4.4	Sensitivities for $C_{el}$ , $L_{el}$ , $R_{el}$ and $U_e$ . . . . .	46
4.5	Circuit diagram for the pulmonary circulation . . . . .	47
4.6	Local sensitivities for the pulmonary circulation . . . . .	48
5.1	(a) Volume and transmural pressure relation (b) ideal electrical capacitor (c) nonlinear residual-charge capacitor (NRCC) (d) sign for NRCC [12] . . . . .	50
5.2	The nonlinear residual-charge capacitor as network [12] . . . . .	51
5.3	Closed and opened circuitry . . . . .	52
5.4	Closed circuitry for the aorta model . . . . .	52
5.5	Individual procedure from measurement of signals to simulation model . . . . .	54



---

# List of Symbols and Abbreviations

---

IVC	Inferior vena cava
SVC	Superior vena cava
PA	Pulmonary artery
TV	Tricuspid valve
PV	Pulmonary valve
MV	Mitral valve
AV	Aortic valve
AoP	Aortic pressure
AvQ	Aortic volume flow
CvP	Central venous pressure
PaP	Pulmonary artery pressure
PvQ	Pulmonary volume flow
ECG	Electrocardiogram
LVP	Left ventricular pressure
RVP	Right ventricular pressure
LVV	Left ventricular volume
RVV	Right ventricular volume
FIR	Finite impulse response
R	Resistance
L	Inductance
C	Compliance
E	Elasticity
P	Pressure
V	Volume
Q	Volume flow
NRCC	Nonlinear residual-charge capacitor



---

# Introduction

---

## 1.1 Motivation

The heart and vessels are part of one of the most important organ systems in the human body, the circulatory system. Problems in this system, due to an unhealthy lifestyle or a chronic disease, can lead to physical constraints or even death. According to the "Global Atlas on Cardiovascular Disease Prevention and Control", an estimated number of 17.3 million people died from cardiovascular diseases (CVD) in 2008 [7]. As a result, CVD represent the main causes for death with a 30% share of all global deaths.

In modern medicine, better understanding of the human cardiovascular system is essential to treat diseases such as cardiac infarctions or inflammations of heart muscles. New approaches such as 4D echocardiography and other types of multidimensional imaging have improved the way to measure and analyze the processes in the human body. However, this examination is limited, due to the fact that research on humans is associated with high cost and risks. Therefore, the use of mathematical models to describe human physiology has increased within the last years thanks to computational power which allows the simulation of complex systems and processes. These models enable a survey of medical problems in a faster, safer and more economic way, as well as gathering of information about the cardiovascular system, which are difficult to detect medically. Furthermore, surgical steps can be calculated and optimized with the knowledge that has been gained through computer models in advance. Nonetheless, the compilation of these models presents a challenge for engineers and medical practitioners because mathematical and physical expertise has to be assembled with physiological knowledge. Both fields have to be matched by finding the optimum between an accurate representation of the physiology and technical feasibility. Accordingly, a close cooperation between these two fields is necessary.

Another issue concerning the compilation of computer models is the requirement of data collection from real processes to train, analyze and evaluate the their quality. Simulation is hardly possible without measured data. As previously mentioned an examination on humans to collect data can be dangerous and, therefore, animal testing is used to get essential information. For the purpose of research in cardiovascular systems, pigs are regarded as suitable because their

circulatory is behaviorally similar to the human one. The values and parameters which have been measured in these tests can be fitted to computer models. These individualized models provide an acceptable quality and performance in simulation. They serve as an environment that helps to determine key values for medical procedures or for the design of medical devices. Pushing this process forward is the ambition for this piece of work.

### 1.2 Content of this Thesis

The objective in this thesis is to find a way how measured data and cardiovascular computer models can be combined, so that the system theory of existing models can be proved. A feasibility analysis is the main focus for this task. In addition to that, a close examination of the system structure with equivalent circuit diagrams will be derived for better analysis. Statistical methods such as the computation of sensitivities will support the investigations.

Chapter 2 introduces the principles of cardiovascular systems with all relevant parameters and signals. The key features of data flow and object-oriented modeling and the basics about the component library *HumanLib* will be highlighted. The library comprises cardiovascular components of the human body and was developed by the department for control engineering at RWTH Aachen University. Additionally, the modeling of tube elements and their analogy to electric circuits will be shown. The theory for sensitivity analysis for parameters in differential equation concludes the chapter.

In chapter 3, an identification of parameters for the aorta model is performed. First, all necessary signals are preprocessed by noise filtering. In a second step, models are extracted from the *HumanLib*, followed by a study of possible input and output configurations. For a better understanding of how real data can be included in the computer models, the *HumanLib* models are disassembled in their basic hydrodynamic elements. The function of these elements is compared to the physical behaviors of the previously introduced analog electrical circuits. Due to the complexity of the differential equations, which both types of elements are based on, the system structure for cardiovascular components and its behavior are explained by matrix notations for four-terminal networks to provide better overview. Moreover, this representation was preferred because the broad theoretical basis for the electrical networks can be applied in this case. The combination of elements, for example, is achieved by matrix multiplications. This way of describing elements leads to a faster and automatized calculation of the differential equations for chosen submodels of the *HumanLib* components. The leading example is the aorta model based on Ursino's research. In addition, the pulmonary circulation serves as a more complex example to prove the approach also realizable for large and complicated structures. The given models in the *HumanLib* are implemented in the object-oriented modeling language Modelica and used in the software tool Dymola. An export to the data flow graphical programming language tool Simulink is necessary to use its parameter estimation toolbox. The interaction of Dymola and Simulink exposes an unexpected error when an acausal systems is exported. This error was considered to be software related and will be discussed shortly. In a detailed analysis for possible configurations of inputs and outputs, the diversity of model structures is revealed. Depending on the configuration, parameters correlate or the relations between input and output become dynamic. Furthermore, the occurring export error can be visualized with the derived matrix representation for the components. The estimation process for parameters of the aorta is carried out with Simulink after aorta model has been exported from Dymola.

Chapter 4 includes an analysis of the system structure for the aorta and the pulmonary circulation by applying a local sensitivity analysis. The model equations are solved, for this purpose, once with the standard setting of parameters and a second time with a variation of a chosen parameter. The difference of both solutions is regarded as sensitivity. Comparing the resulting deviation with other sensitivities helps to define the relevant parameters in the system.

In Chapter 5, the conclusion for the previous chapters is drawn by discussing the results and comparing the models with other studies. Furthermore, suggestions for improvements and limitations for measurements and computer models are pointed out in this part of the thesis.

As a conclusion, the last chapter contains the prospects and chances for future projects of the presented approaches.



---

# Medical, Physical and Mathematical Background

---

The following part presents fundamental principles which are relevant for modeling of the human cardiovascular system. Furthermore, basics about object-oriented and dataflow programming are provided to show how the described physiological processes can be implemented in computer software. The results of this implementation are computer models which are essential for simulation experiments. In addition to that, parameters which appear in the models can be determined during an identification process. How this process works is explained and a library of models, which is called *HumanLib*, has been developed at the IRT in previous projects and the underlying theory will be presented [2]. The thesis is mainly based on this library and will elaborate on its functionality. Finally, the last subchapter highlights a mathematical method which includes the local sensitivity of the model parameters and which will be applied for an exemplary experiment.

## 2.1 Principles of the Human Cardiovascular Physiology

The cardiovascular system has the function to supply all organs and parts of the human body with blood. The complex structure of the system can be simplified by a description with three components: blood, vessels and heart. Blood includes cells, which are able to carry substances and exchange them with organs. The blood transports these cells contained with oxygen from the lungs to organs and carry carbon dioxide and other byproducts of metabolism from organs to the lungs. This way of supplying can be regarded as a flow process with the blood as transport medium. For further calculations blood is considered to be a Newtonian fluid with constant density. Additionally, the flow processes are considered to be laminar which means that the blood flows in longitudinal direction. The wall material is homogeneous and isotropic. Each component has a constant cross sectional area.

Blood is transported in vessels, which are tubular elements. Vessels run through the body to connect heart and lungs with all other organs. There are three different types of vessels: veins, arteries and capillaries. Veins carry blood to the heart, whereas arteries lead it away from it. Capillaries are very small blood vessels, which are structured in networks surrounding organs and tissues and supply them with oxygen and other sustenances.

For a hydrodynamic consideration complex organs such as the lungs can be treated as a network of vessels. This network is called pulmonary circulation. Furthermore, all other blood vessels, which supply organs in the human body, can be summed up in the systemic circulation. In doing so, the organs are structured in a parallel arrangement. The human heart is a composition of muscles and valves and comprises a left and a right half. Each half, consisting of an atrium and a ventricle, serves in its function as a pump. The pressure build-up in this pump is generated by alternating contraction and relaxation of the surrounding muscles. Figure 2.1 shows the described constellation of the four cardiac chambers and the anatomy of the heart. Blood

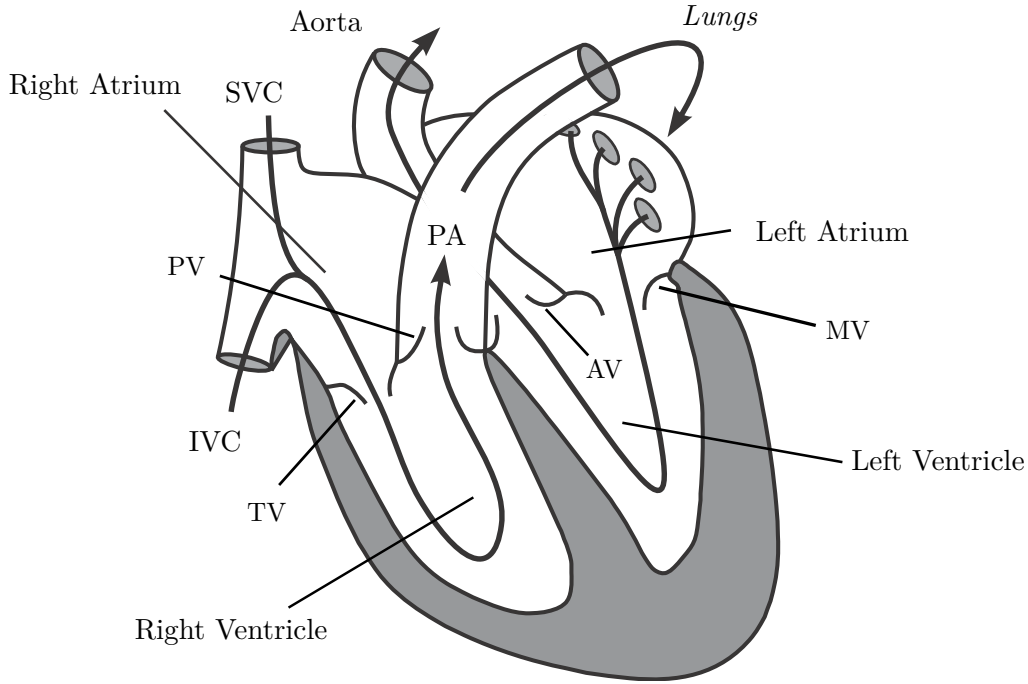


Figure 2.1: Anatomy of the heart [6]

enters the right atrium via the superior vena cava (SVC) and the inferior vena cava (IVC) and is led in the right ventricle. From there blood is pumped into the pulmonary artery (PA) and passes the pulmonary circulation. It reenters the heart through pulmonary veins and passes from the left atrium to the left ventricle. In the left ventricle high pressure is built up and the blood is ejected to the aorta and streams from there through the systemic circulation.

There are four valves in the human heart. The tricuspid valve (TV) and the pulmonary valve (PV) are part of the left cardiac half. The mitral valve (MV) and the aortic valve (AV) belong to the right half.

The right half pumps blood in the pulmonary circulation, whereas the left half pumps it in the systemic circulation. Therefore, the human cardiovascular system can be described as a series connection of the pulmonary circulation, the left cardiac chambers, the systemic circulation and the right cardiac chambers as shown in figure 2.2.

By analogy with electrical circuits, flow processes such as the cardiovascular system can be determined by the flow resistance, the hydraulic inductance and the compliance of pipe systems. The resistance can be calculated from the pressure difference  $\Delta P$  and the volume flow  $Q$ :

$$R = \frac{\Delta P}{Q} = \frac{P_{in} - P_{out}}{Q} \quad (2.1)$$

$P_{in}$  represents the incoming pressure, whereas  $P_{out}$  defines the pressure of the outflowing stream.  $Q$  is both, the volume flow of the inflowing and outflowing stream. This equation helps to



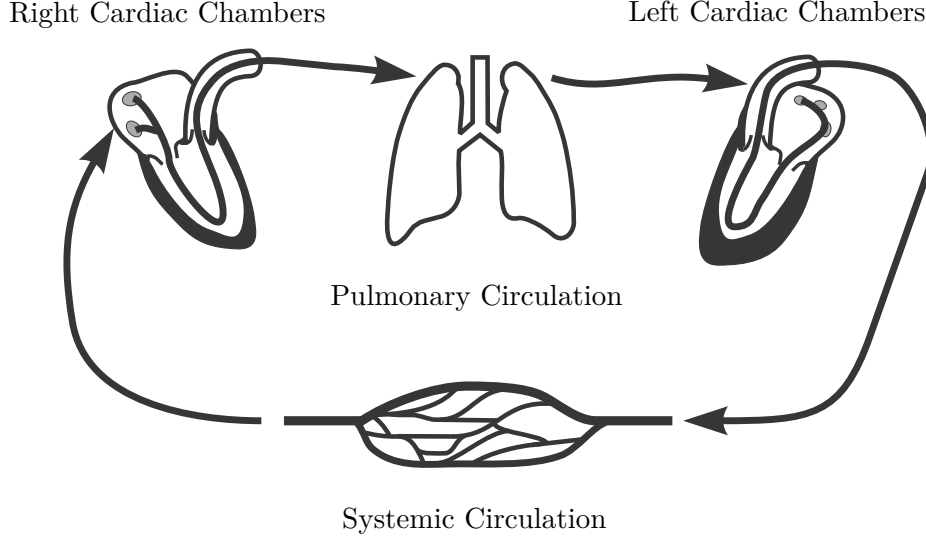


Figure 2.2: Cardiovascular system [6]

understand the pressure level in the ventricles. The left ventricle has to build up pressure for the systemic circulation, which consists a number of organs in parallel arrangement. Because of the analogy to electric circuits, the same physical considerations and laws like used for electronic parts can be applied. With Kirchhoff's and Ohm's law the resulting resistance for the any circulation can be computed by

$$R_{res} = R_1 + R_2 + R_2 + \dots \quad (2.2)$$

for series connection and

$$R_{res} = \frac{1}{\frac{1}{R_1} + \frac{1}{R_2} + \frac{1}{R_2} + \dots} \quad (2.3)$$

for parallel connection. The resistances of single organs are  $R_1$ ,  $R_2$  and  $R_3$ . It shows that  $R_{res}$  increases as more organs are connected in series. The systemic circulation consist of many organs in parallel and series connection and the left ventricle has to overcome the resulting resistance. On the other hand, the right ventricle maintains the pressure of the pulmonary circulation, which consists of the lungs. The resistance is smaller in comparison to the one for the combination of many organs in the systemic circulation. As a result, the pressure in the left ventricle is higher than the pressure in the right.

The hydraulic inductance  $L$  of a pipe or a vessel can be determined by the derivative of the volume flow  $\dot{Q}$  and the pressure difference  $\Delta P$ :

$$L = \frac{\Delta P}{\dot{Q}} = \frac{P_{in} - P_{out}}{\dot{Q}} \quad (2.4)$$

Acceleration and deceleration cause inertia in the pipe system. Similar to the inertia in mechanical systems, the hydraulic inductance defines the pressure differences  $\Delta P$  for a the acceleration and deceleration of a volume  $Q$ .

The compliance  $C$  of a vessel is the reciprocal value of the vessel's elasticity  $E$ . The compliance represents the vascular ductility and can be determined by:

$$C = \frac{1}{E} = \frac{\Delta V}{\Delta P_{tm}} \quad (2.5)$$

$\Delta P_{tm}$  is the transmural pressure, which is the difference between the intravascular and extravascular pressure.

$$\Delta P_{tm} = P_i - P_e \quad (2.6)$$

The intravascular pressure can be measured inside of the vessel, whereas the extravascular pressure is applied from outside of it. Extravascular pressure can be the atmospheric pressure or can be caused by external forces. Similar to the conductivity in electric circuits the compliance specifies the ability to store. An easy calculation shows that a positive transmural pressure and compliance means a positive difference of volume in equation 2.5. This volume difference embodies the volume which has been stored in the vessel [3], [14]. The pressure and volume flow in the left heart is shown in figure 2.3. One cardiac cycle is defined as one heartbeat starting The cardiac cycle is divided into the systole (Sys) and the diastole (Dias). During the systole the heart contracts and ejects blood into the aorta, highlighted by a gray background in the figure. The relaxation and filling is part of the diastole.

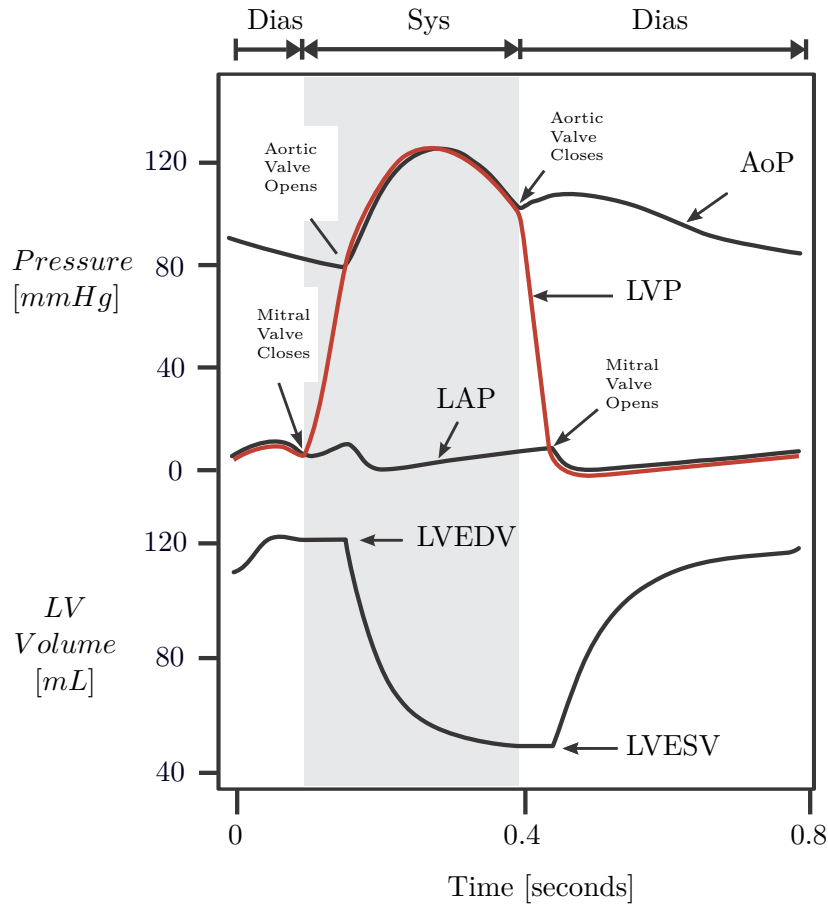


Figure 2.3: Cardiac cycle for the left ventricle in the human body [6]

In figure 2.3 the pressure for the left ventricle (LVP) rises as soon as the mitral valve closes. After some time the aortic valve opens and the blood flows into the aorta. The pressure in the aorta (AoP) is very close to the left ventricle pressure just until the aortic valve closes again. After that, the pressure falls until the mitral valve opens again. The pressure in the left atrium (LAP) hardly varies during the cardiac cycle in comparison to the others. In the figure, the volume in the left ventricle is plotted for the cardiac cycle. Two typical values are marked. The left ventricular end-diastolic volume (LVEDV) is the maximum volume, whereas the left ventricular end-systolic (LVESV) is the minimum volume reached during one cycle.

## 2.2 Data Flow and Object-Oriented Modeling

To describe the physiology of human cardiovascular systems it is necessary to build up a computer model of the organs and parts of body. A computer model is a reproduction of the real system on a computer to simulate its behavior. A useful software tool for these purposes is Matlab/Simulink®, which is based on data flow programming. A function block in Simulink has an unidirectional data flow and defines an input  $u$  and output  $y$  of a system. The relation between input and output is defined by the block, which consists of parameters  $p$  and state variables  $x$ .

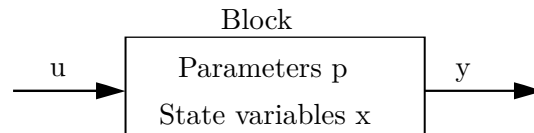


Figure 2.4: Simulink block function

The output  $y$  is defined by

$$y = f(t, x, u, p) \quad (2.7)$$

The parameters  $p$  are not time-dependent, but state variables  $x$  and inputs  $u$  can vary over time. Multiple inputs and outputs are possible and all signals can be processed dimensionless. Another approach to create models is based on the object-oriented language Modelica. Object-oriented modeling means to build up physical objects and define a relation to the other objects. This method resembles a modular concept. Differential equations, which describe the physical behavior of processes in the real system, determine the physical objects. The relation is created by connecting the physical objects in a way that it represents the real system. A simple example of an object-oriented model is highlighted in figure 2.5. The model shows a tank system including the three physical objects of a tank. Variable such as pressures  $P$ , water levels  $H$  and volume flows  $Q$  are properties of each tank and change over the time. With a simulation of an implemented model the progress of the variable can be computed. All object are based

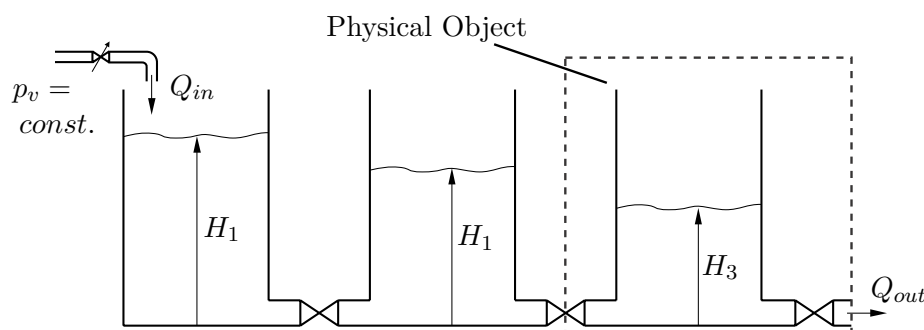


Figure 2.5: Model of three tanks [1]

on hydrodynamic equations and are connected to each other. Similar to the Kirchhoff's circuit laws, there are conditions, which have to be fulfilled in the connections of the tanks.

For the volume flow one is

$$\sum_{i=1}^n Q_i = 0 \quad (2.8)$$

in every connection. This means that all incoming flows are equal to the outgoings and there is no loss of volume in the connection.

For the pressures the equation is

$$P_1 = P_2 = \dots = P_n \quad (2.9)$$

These two master equations are essential for object-oriented modeling and simulation experiments. For building up a model, physical objects, like a tank, can be taken from a library, which provides a number of standard components. These components are connected and form the structure of the whole model. Advantages of object-oriented modeling is the overview about the model and the structural and graphical similarity to the reality. All variables are encapsulated in the objects and only appear inside of it. Furthermore, it is possible to change objects without destroying the structure of the whole model. A tank could easily be replaced by a pump or another hydrodynamic object, for example. Eventually, complex model behavior can be structured by a hierarchical arrangement. Therefore, the model remains understandable even with many subdivisions. A common software for object-oriented modeling is Dymola, which is equipped with a large library of components such as electrical and mechanical objects. Considering the example of the tank system, the graphical representation of the Simulink model is shown on following figure 2.6. The model equations have been linearized to provide a simple model structure and a better overview.

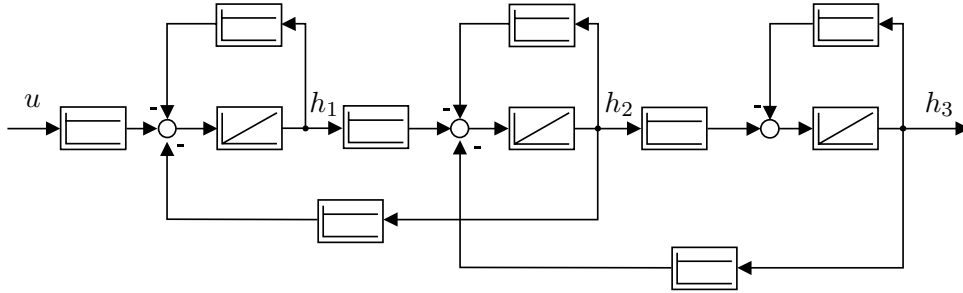


Figure 2.6: Graphical representation of a Simulink model of the three tank system [1]

The model composes of integral and proportional elements, a defined input  $u$  and an output  $h_3$ . Although it represents the similar output behavior like the object-oriented model, its structure is unintelligible. Furthermore, the input and output configuration is fixed and has to be determined in advance. Therefore, a simulation with this model is limited to changes in the configuration and new requirements could lead to an uselessness of the model [1].

## 2.3 Identification of Parameters in Computer Models

The objective of an identification is to build up a mathematical model of a process so that the resulting error between process and model approximates a minimum. For this procedure the input signal  $u$  and output signal  $y$  of the process have to be measured. Before these measured signals can be used, a preprocessing of the data is often necessary. In real processes the output signal is superimposed by a noise signal  $n$ . The difference between the modeled and real outgoing signal  $y_m$  and  $y$  is the error signal  $e$ . Figure 2.7 shows the procedure of an identification. The analysis, which is also called optimization in the following, suggests a change in the model so that the error becomes smaller [1]. In this thesis the focus is on parameter identifications, which are also called parameter estimations. A parameter estimation requires a model which consists of ordinary differential equations including parameters and, therefore, good knowledge about the process is needed in advance. During the identification the model parameters are estimated, the outgoing signal  $y_m$  is simulated and the error is computed. In the next step

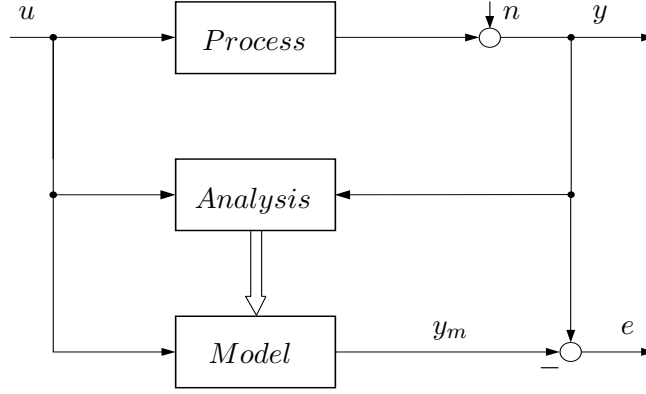


Figure 2.7: Identification of a process [1]

an optimization algorithm calculates and suggests how the parameters have to be changed for minimizing the error. Therefore, the identification can be considered as an iteration with the two steps simulation and optimization. In this thesis Simulink's estimation toolbox is used to estimate parameters.

### 2.3.1 Simulation

Simulink contains a number of solving algorithms for the simulation of models. Each solver determines the next step in time and applies a numerical algorithm which solves the underlying differential equation. The result is the progress of the model output  $y_m$  for the predefined input  $u$ . Depending on the chosen algorithm, accuracy requirements can be specified. Therefore, the choice of solver has a high effect on the simulation results. Generally, solvers can be divided into fixed-step and variable-step algorithms. For fixed-step solvers a step size has to be predefined by the user and remains constant during the simulation. Among others, Simulink provides fixed-step solvers based on Euler's method, Heun's method and the Bogacki-Shampine formula. Variable-step algorithms vary the step size during the simulation from step to step. The most common variable-step solver is based on the Dormand-Prince algorithm. Both types of solver have advantages and disadvantages and the choice of algorithm also depends on the model and its differential equations. For the following estimation procedure, solver will be specified according to the model structure.

### 2.3.2 Optimization

After a complete simulation, an optimization of the model output is applied. During optimization parameters in the equations are varied in order to fit the computed model output  $y_m$  to the desired or real output  $y$ . In other words, the difference between computed and real output, which is defined as error signal  $e$ , is minimized by each step. For this purpose a cost function is derived including the error  $e$ . Cost functions can be the sum squared error or the sum absolute error.

The optimization methods minimize this cost function  $Q$ . A very common Simulink method uses the "nonlinear least squares", which minimizes the sum of squared errors. The optimization procedure with this algorithm for  $N$  data points can be summarized as

$$Q = \frac{1}{N} \cdot \sum_{n=1}^N e_n^2 \rightarrow \min \quad (2.10)$$

This algorithm will be used for all estimations in this thesis. In addition to the optimization method, constraints and bounds for the estimated parameters can be defined in advance. For example, it is possible to define a lower and upper boundary for a parameter. After each optimization procedure, the new model is built up and the a new simulation starts. This iteration is stopped by predefined termination condition. Further information can be taken from Matlab's documentation for the parameter estimation toolbox which is provided on Mathworks website for each Matlab version [1].

## 2.4 Components and Models in the *HumanLib*

In recent projects of the Institute of Automatic Control at RWTH Aachen University new approaches have been developed for modeling cardiovascular systems. Based on object-oriented modeling, the component library *HumanLib* has been developed in Anja Brunberg's dissertation. Based on the explained equations (2.1) to (2.5) and the research by Mauro Ursino, an implementation in Dymola has been carried out. The result is a cardiovascular system, which simulates the blood flow of the whole body and processes in the nerve system. The focus of this thesis is on the model and parameters of Ursino's research [13].

The graphical representation is given in figure 2.8.

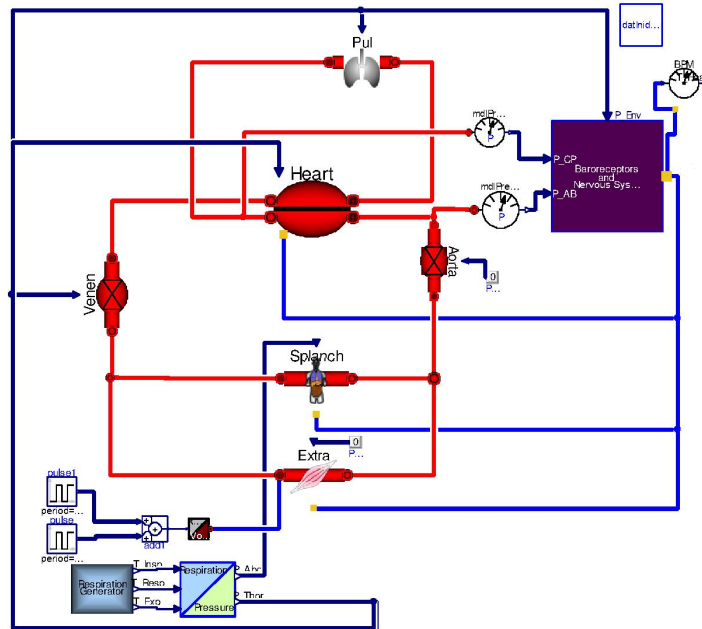


Figure 2.8: *HumanLib* model based on [13]

The entire model is based on the previous mentioned objects for the flow resistance, the hydraulic inductance and the compliance of vessels. Figure 2.9 shows the graphical representation for the three objects. The library enables the modularity of systems by connections. Each system can be composed of the objects with individual parameters. This makes it possible to simulate the behavior in parts of the body. Figure 2.8 shows the model of the complete cardiovascular system.

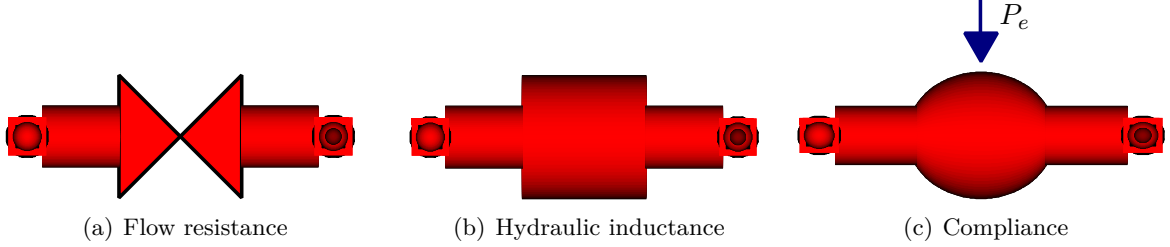


Figure 2.9: Basic objects in the *HumanLib*

The following investigations deal with the three basic objects. All processes in the block for the baroreceptor and the nerve system and its effect on the hydraulic components are neglected in the following approaches.

## 2.5 Tube Element and the Equivalent Circuit Diagram

In the human body vessels can be regarded as elastic pipes. These pipes can be described by wave equations, which explain the change of pressure  $P$  and volume flow  $Q$  in the element.

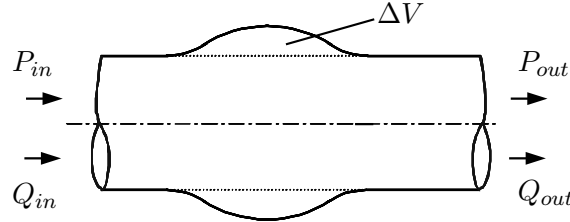


Figure 2.10: Tube element [4]

By analogy with electrical systems the behavior in elastic tubes can also be modeled as a circuit like shown in figure 2.11. In this model the voltages  $U_1(t)$  and  $U_2(t)$  correspond to the incoming and outgoing pressures. The current flows  $I_1(t)$  and  $I_2(t)$  resemble the volume flows.

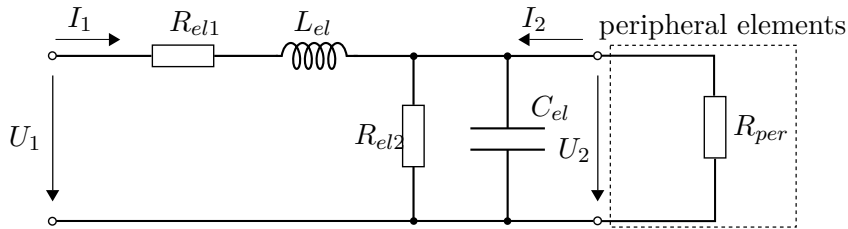


Figure 2.11: Equivalent Circuit Diagram [4]

All voltages and currents are time dependent. The three elements resistor, inductor and conductor can be found in the diagram with the labels  $R_{el}$ ,  $L_{el}$  and  $C_{el}$ . The equation for each element

is similar to the hydraulic calculations 2.1 to 2.5. Table 2.1 summarizes the relation between electric and mechanical signals. With the Kirchhoff's circuit laws two differential equations

Physical quantity	Symbol	Units	Electric analogs	Symbol	Units
Pressure	$P$	$mmHg$	Voltage	$U$	$V$
Volume flow	$Q$	$\frac{ml}{sec}$	Current	$I$	$A$
Volume	$V$	$ml$	Charge	$Q_{el}$	$C$
Viscous resistance	$R$	$\frac{mmHg \cdot sec}{ml}$	Electrical resistance	$R_{el}$	$\Omega$
Elastic compliance	$C$	$\frac{ml}{mmHg}$	Electrical capacitance	$C_{el}$	$F$
Inertance	$L$	$\frac{mmHg \cdot ml}{sec^2}$	Inductance	$L_{el}$	$H$

Table 2.1: Electromechanical relations

can be formulated. For a better use and analysis of the equations, a Laplace transformation is applied.

$$U_1(t) - U_2(t) = -R_{el1} \cdot I_1(t) - L_{el} \cdot \dot{I}_1(t) \quad \circ \bullet \quad U_1 - U_2 = (R_{el1} + L_{el} \cdot s) \cdot I_1 \quad (2.11)$$

$$I_1(t) + I_2(t) = \frac{1}{R_{el2}} \cdot U_2(t) + C_{el} \cdot \dot{U}_2(t) \quad \circ \bullet \quad I_1 + I_2 = (\frac{1}{R_{el2}} + C_{el} \cdot s) \cdot U_2 \quad (2.12)$$

These equations indicate the same structure as the wave equations, which describe the physical states in a flexible tube element. Further calculations and studies about models with tube elements can be found in literature such as [4]. In comparison to the assumptions in the referred literature, the models and equations are not based on a propagation path but only on the time. Therefore, the discussed calculations are similar to approaches in acoustic studies. These and further electromechanical analogies can be found in [11]. The presented equivalent circuit diagram will be used in the chapter 3 and 4 to examine the calculations with different configurations of inputs and outputs.

## 2.6 Sensitivity analysis of parameters

In order to evaluate the model structure, the effect of a parameter variation exposes important information. The method of variation also determines, which sensitivity the differential equation reveals concerning a chosen parameter. Therefore, a mathematical analysis enables to identify critical parameter dependences. The parameter's sensitivity can be computed in their local area or globally. A local consideration is the focus in the following part.

### 2.6.1 Local sensitivity analysis

Generally, a local sensitivity can be computed by deriving the solution  $y(t, p_i)$  for the differential equation with respect to the parameter  $p_i$ . The vector  $Z$  is called sensitivity matrix and composed of derivation with respect to each parameter.

$$Z = \frac{\partial y(t, p_i)}{\partial p_i} \quad (2.13)$$

Standard rules of differentiation are usable for this case. As the structure of  $y$  is not always clear and the parameters are deeply encapsulated in the equation, the method can become difficult.



Alternatively, the internal numerical differentiation method can be used to obtain the vector  $\mathbf{Z}$ . For this method a variance is superimposed to the original value of the chosen parameter  $p_i$ .

$$p_{i,new} = p_i + \alpha_i \quad (2.14)$$

$p_{i,new}$  is parameter and  $\alpha_i$  is the increment for each parameter. For very small increments, the derivatives can be approximated:

$$\frac{\partial y(t, p_i)}{\partial p_i} \approx \frac{y(t, p_{i,new}) - y(t, p_i)}{\alpha_i} \quad (2.15)$$

For the choice of  $\alpha_i$  literature suggests a value of  $\alpha_i \approx \sqrt{ACC}$ , where  $ACC$  is the relative accuracy defining how precise the function  $y(t, p_i)$  can be computed. In engineering applications like finite element calculations,  $ACC$  is approximately  $10^{-3}$ . Alternatively, it is  $10^{-16}$  in double precision IEEE arithmetic. More information can be taken from literature [10].



---

## Identification of Parameters in Models with Measured Data

---

In the following chapter an identification of chosen parameters will be applied with partial models of the *HumanLib*. A set of measured data is selected and undergoes a preprocessing procedure before parameters can be identified. Valid data will be divided and chosen and necessary adjustments to the model inputs and outputs have to be carried out. In a second step the Dymola models have to be prepared according to the desired estimation of parameters. First, the model structure is reduced and inputs and outputs have to be determined. Later, the Dymola models are exported to Simulink to use its estimation toolbox and identify parameters. For the estimation procedure the previously prepared data are used as inputs and outputs. During the estimation numerical simulation and optimization adjust the parameters so that the simulated output fits to the given measured data. Eventually, all estimation results are plotted and gathered for a later discussion with literature values for the considered parameters.

### 3.1 Preprocessing of Measured Data

For an identification of parameters the measurement of signals is necessary. The databases used in this thesis derives from testings on domestic pigs. These have been proved to be suitable for cardiac measurements because of their anatomic similarity to the human cardiovascular system. The data set composes the following ten signals:

- Aortic pressure (AoP)
- Aortic volume flow (AoQ)
- Central venous pressure (CvP)
- Pulmonary artery pressure (PaP)
- Pulmonary volume flow (PvQ)
- Electrocardiogram (ECG)
- Left ventricular pressure (LVP)
- Right ventricular pressure (RVP)
- Left ventricular volume (LVV)
- Right ventricular volume (RVV)

Figure 3.1 gives an overview of the points where the signals were measured. The method of measurement remain unconsidered for the following examinations and, therefore, will not be described. The record duration is 243.5 seconds and the sample rate is 2000 Hz. The number

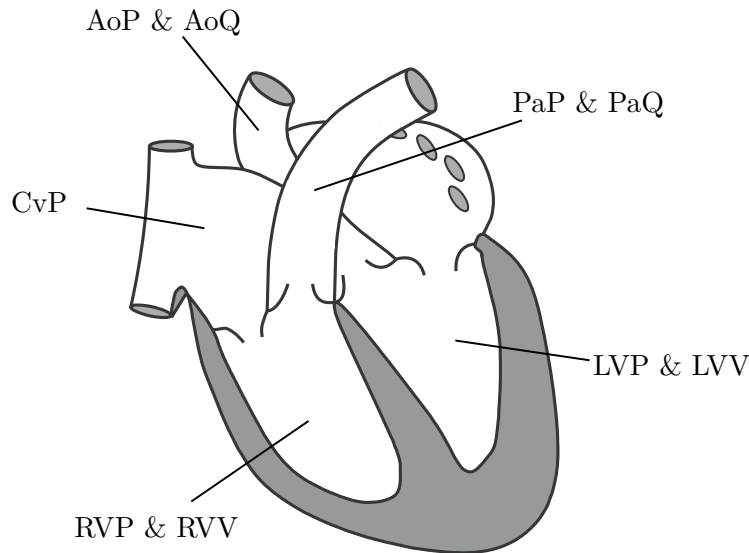


Figure 3.1: Points of measurement [6]

of data points amounts  $3.94 \cdot 10^6$  for all signals,  $394 \cdot 10^3$  for each. All pressures are recorded with the unit millimeter of mercury (mmHg), all volume flows as liters per minute (L/min).

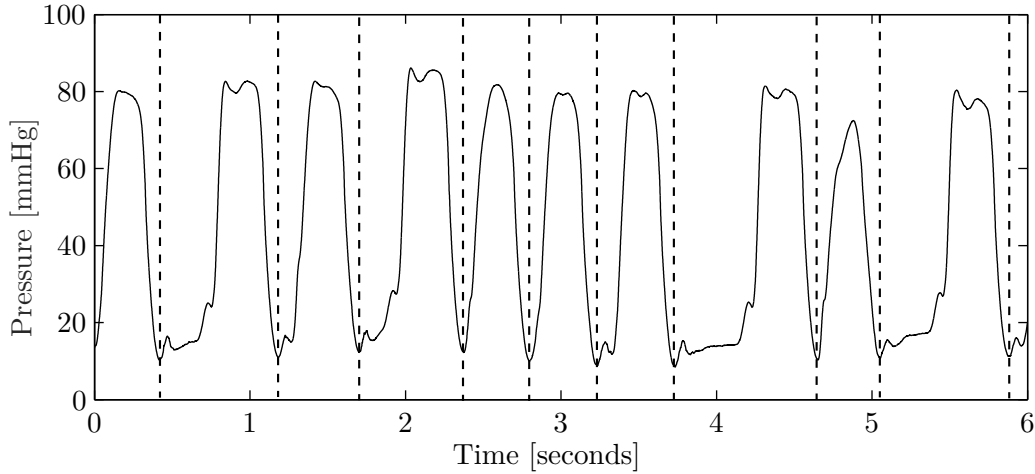


Figure 3.2: Measured signal LVP

On the shown diagram 3.2 the LVP is plotted in mmHg against the time in seconds. The signal is unfiltered and includes all kind of measurement deviations such as outliers and noises. However, a repeating pattern can be found starting and ending at the local minimums. The minimums are located at the time when the mitral valve closes and, therefore, can be chosen as a starting point for the cardiac cycle. The waveform indicates a characteristic shape for all windows, which are separated by dotted lines. The duration of the cardiac cycles varies from about 0.3 to 0.9 seconds.

For a better understanding the methods of preprocessing will be presented with a selection of signals. The pressure and volume flow in the left ventricle and aorta are important for the upcoming procedures and, in addition, a comparison of the measured signals with literature values can be carried out with good precision. Therefore, the signals LVP, LVV, AoP and AoQ will be highlighted in the following. A closer look on a sequence of 6 seconds for the signals

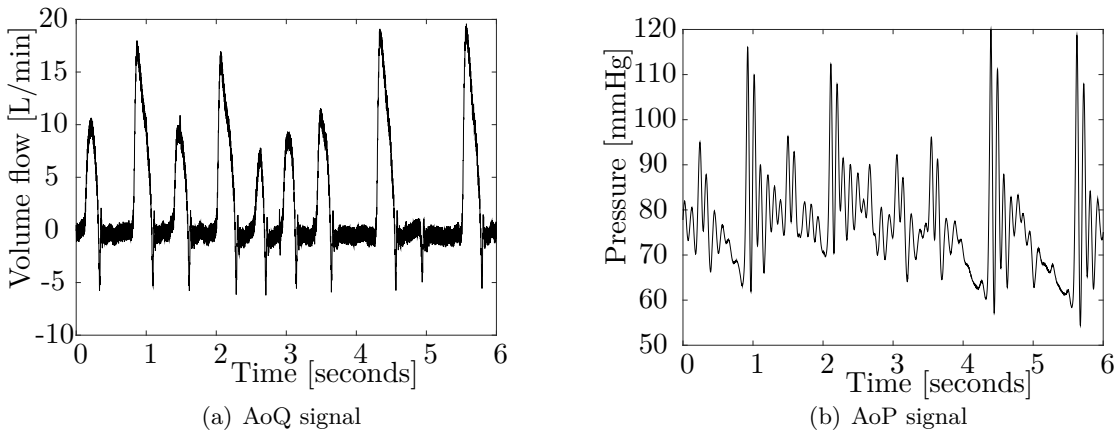


Figure 3.3: Unfiltered signals with noise

AoQ and AoP in figure 3.3 shows the unsatisfactory quality of the measurements. The AoQ signal is superimposed by noise with a high frequency of about 140 Hz, which can be detected by extremely high fluctuations resulting in a dense line between every characteristic peak. The amplitude of noise is relatively small with an absolute value of about 0.75 L/min. The AoP signal features a similar noise but frequency and amplitude differ compared to the signal for the volume flow. Here, a frequency of about 20 Hz can be detected for the noise. Its amplitude

varies and features a range of about 2 to 25 L/min. As described in chapter 2 the behavior of pressure and volume flow cardiac cycle for humans theoretically looks like highlighted on figure 2.3. The measured signals are shown in figure 3.4 for a time interval of 3 seconds. It can be stated that the noise falsifies the signal in a way that the expected characteristic behavior can not be identified.

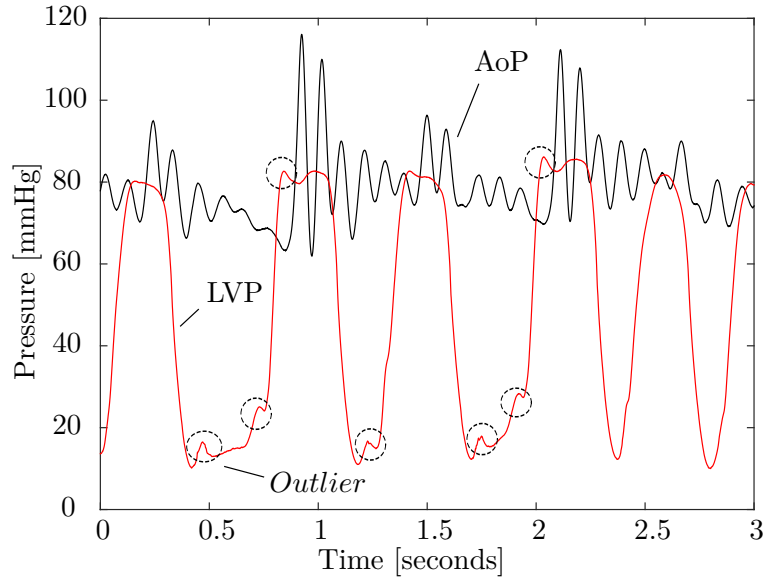


Figure 3.4: AoP and LVP signals

The LVP signals includes outliers and anomaly behavior such as peaks after each cardiac cycle marked in the figure. Emphasizing these three signals, a preprocessing of the measured data is necessary. By filtering the signals, outliers and noises can be removed and, therefore, will be applied before further calculations are performed.

Additionally, the LVP signal has to be transformed to a volume flow because the used Dymola and Simulink models run on equations which compute the flow signals. The resulting volume flow in the left ventricle will be determined as LVQ in the following.

### 3.1.1 Filtering of signals LVP, AoP and AoQ with a finite impulse response filter

As filtering methods the finite impulse response filter (FIR), will be presented in the following.

The application of the filter will be shown for the signals LVP, AoP and AoQ with a suitable setting for each. For discrete signals such as given measured data, Matlab provides the functionality to use a finite impulse response filter (FIR). The filtering algorithms guarantees that the filters impulse response settles to zero in a finite time interval, which means that it is stable. For an application a filter `filt` is determined, which is set up by the function `designfilt`.

While `N` defines the order of the lowpass filter, the parameters `fpass` and `fstop` determine which frequencies can still pass and which will be stopped.

The setting for these parameters which give a suitable filtered outcome for each signal is given in table 3.1. The sample rate `fs` is 2000 Hz for each. In figure 3.5 the unfiltered and filtered

Signal	N	fpass	fstop
LVP	400	1	10
AoP	300	0.1	10
AoQ	200	0.1	10

Table 3.1: FIR setting

signals are illustrated. It can be shown that the first recorded data points are set to zero due to the delay caused by the FIR filter. For the LVP the first 200, for the AoP signal the first 150 data points are zero. For the AoQ signal this phenomena seems to be irrelevant as the first entries are zero anyways. By comparison of table 3.1 and the delay, it is coherent that both values correlate. For further calculations the first recorded seconds will not be used.

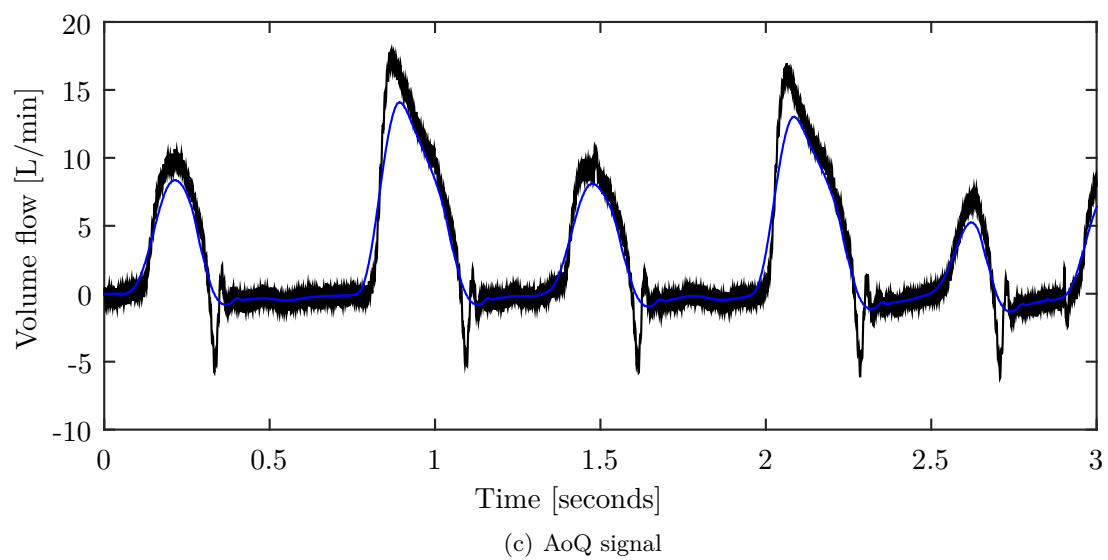
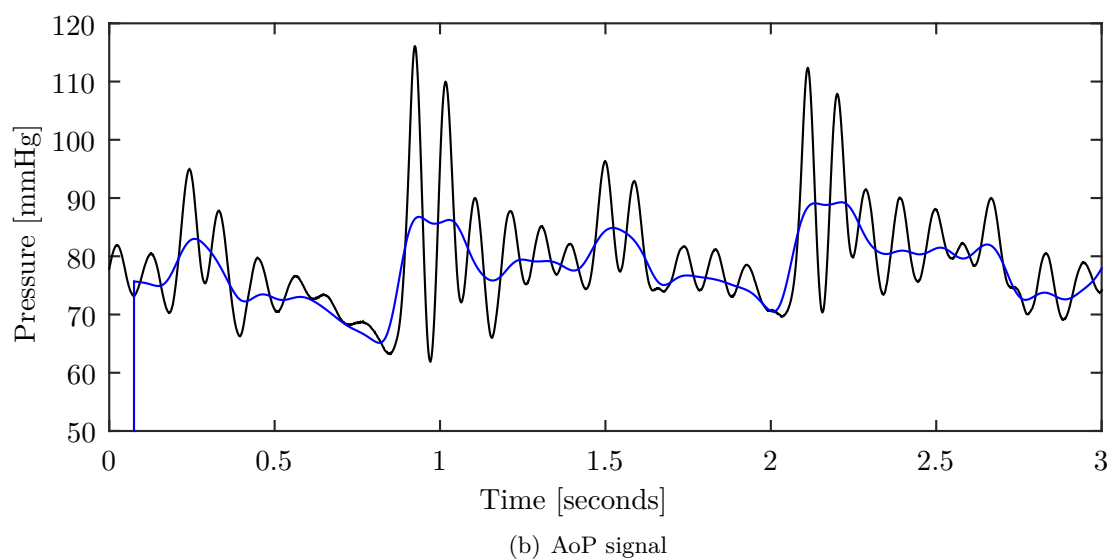
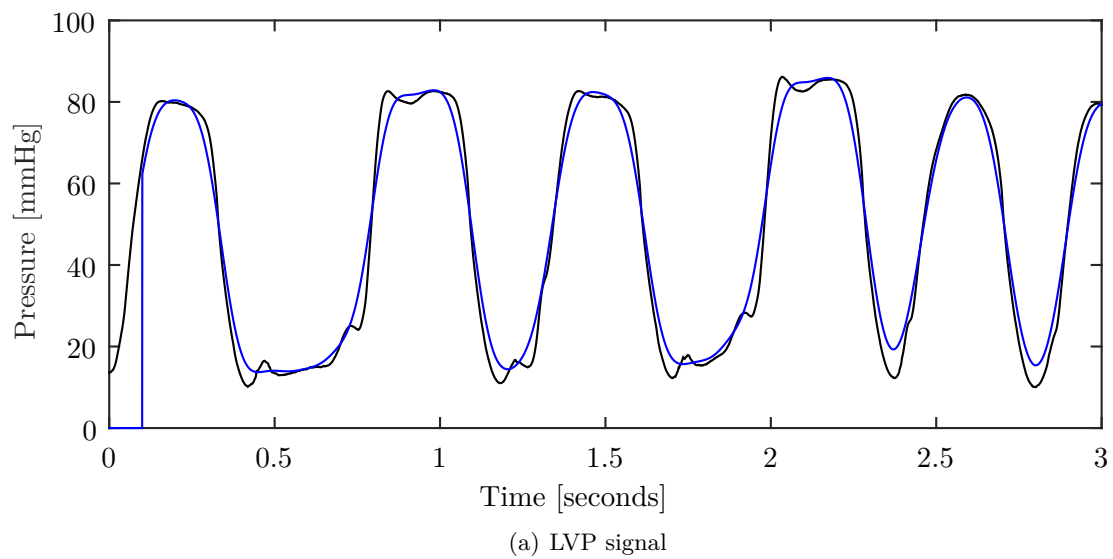
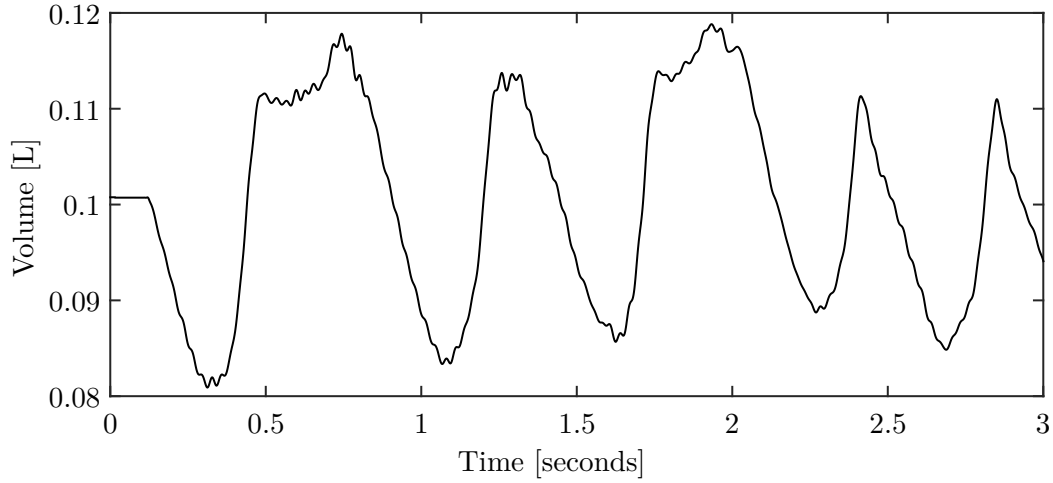


Figure 3.5: Unfiltered and filtered signals LVP, AoP and AoQ using a FIR filter

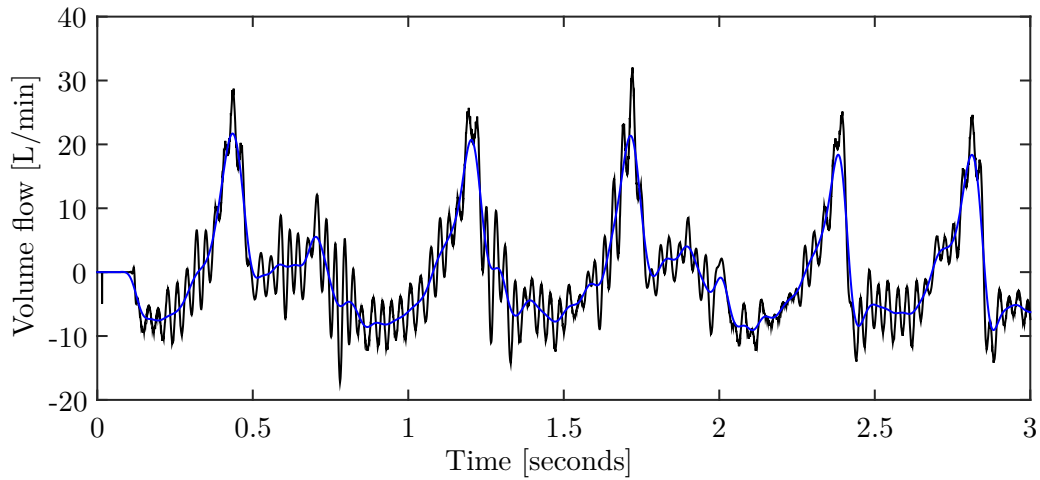


## 3.1.2 Transformation from LVV to LVQ and filtering

To transform a volume to a volume flow, the signal for the volume has to be derived. As an example, LVV will be transformed to LVQ in the following section. Determining the derivatives of signal with a high sample rate and a resulting high number of data points can effect an amplification of the noise as shown in figure 3.6. Therefore, the signal has to be filtered as discussed before.



(a) LVV signal



(b) unfiltered and filtered LVQ signal

Figure 3.6: Transformation from LVV to LVQ

The filter order  $N$  was set to 300. The frequencies are 0.1 for `fpass` and 30 for `fstop`. Considering both diagrams shows that the resulting volume flow LVQ is the flow which enters the ventricle. Assuming that there is no loss of volume flow in the ventricle and neglecting inertia, the negative LVQ signal will be used as outgoing volume flow from the ventricle.

## 3.2 Preparation of Models

The *HumanLib* is composed of three cardiovascular models based on the researches of Ursino and Leaning. For the parameter estimation in this thesis the structure of the model by Ursino serves as the basis for the identification. This section will explain how equations can be derived from the models and represented in matrix notation. Solving these equations in combination with feeding them measured data will lead to a determination of chosen parameters. For this purpose the model will be separated into basic Dymola elements and, later, exported to Simulink for identification procedures. First, inputs and outputs have to be defined and a study about possible configurations will be provided because optimization processes during the estimation of occurring parameters have to be adjusted depending on which inputs and outputs are chosen. The interaction between both used software tools Dymola and Simulink implies a challenging task. Before exporting, the elements have to be modified to avoid software based export errors. Conclusively, the prepared models are ready for the identification.

As examples, the aorta and the pulmonary circulation will be presented. The aorta can be modeled as any other vessel and, therefore, features a very simple structure. To verify that the matrix notation is also applicable for more complex structures, the mathematical equations for the pulmonary circulation are derived in the final step.

### 3.2.1 *HumanLib* elements as electrical four-terminal network

The *HumanLib* provides complete full body models for the cardiovascular system and simulations can be executed. However, the graphics and equations in Dymola make it difficult to understand the behavior of single elements in the model. Cutting out a part such as the aorta from the full body model results in a complicate and unclear representation. Therefore, another approach to describe the model structure is needed.

The three elements resistance, inductance and compliance can be analyzed and illustrated as electrical four-terminal network. These networks have four poles or terminals and can be connected with other network. For each element there is one defined four-terminal network with inputs and outputs, shown in table 3.2. As the elements are composed of the linear electrical components resistor, inductor and compliance, the shown networks are linear and passive. The resulting resistance and inductance are based on the same equations like in the *HumanLib*. For the compliance it is assumed that the external pressure is neglected and, therefore, set to zero. A mathematical description with matrices is possible and will be used in the following to analyze the structure of compositions of the three elements. In the table the  $A$  matrices are given for

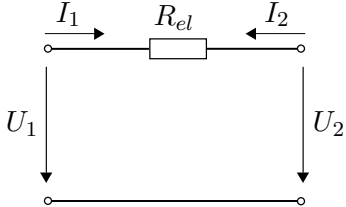
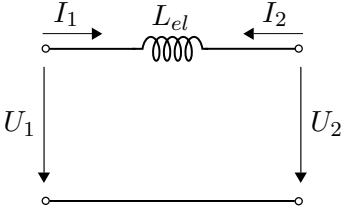
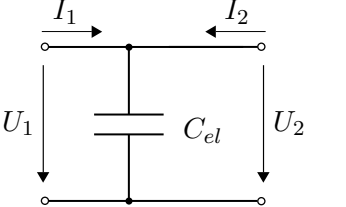
Resistance	Inductance	Compliance
 $A_R = \begin{pmatrix} 1 & R_{el} \\ 0 & 1 \end{pmatrix}$	 $A_L = \begin{pmatrix} 1 & L_{el} \cdot s \\ 0 & 1 \end{pmatrix}$	 $A_C = \begin{pmatrix} 1 & 0 \\ C_{el} \cdot s & 1 \end{pmatrix}$

Table 3.2: Resistance, inductance and compliance as electrical four-terminal network

each element. The relation between input and output is

$$\begin{pmatrix} U_1 \\ I_1 \end{pmatrix} = \begin{pmatrix} 1 & L_{el} \cdot s \\ 0 & 1 \end{pmatrix} \cdot \begin{pmatrix} U_2 \\ -I_2 \end{pmatrix} \quad (3.1)$$

$$A = \begin{pmatrix} a_{11} & a_{12} \\ a_{12} & a_{22} \end{pmatrix} \quad (3.2)$$

while  $U_1$  and  $I_1$  are chosen as inputs. Parallel and series connection can be built up and calculated by matrix algebra. Thus, even complex models such as the pulmonary circulation can be analyzed with a compact matrix representation. For calculations with four-terminal network refer to the literature [15].

### 3.2.2 Export to Simulink

For exporting a model, Dymola offers the functionality to compile it as a program, which is called Dynamic Model Simulator (Dymosim). This resulting file can be run by other software tools. Simulink provides a function block which runs the Dymosim application and which can be implemented in a standard Simulink model.

Dymola indicates an error during the compilation of the code as soon as the input signal is derived in the model. As the simplest example for the error occurs when using the derivative block "der()" and connecting them with a "RealInput" and a "RealOutput", shown on figure 3.7. As earlier mentioned, the reason for this error is the acausality of the system. The derivative block is physically not realizable, as it needs future input data.

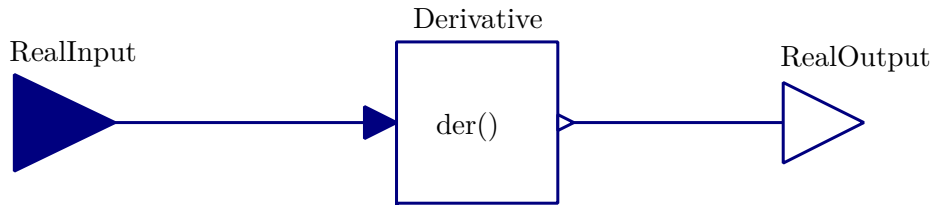


Figure 3.7: Dymola model with a derivative block

The model in figure 3.7 is not compilable. Therefore, the following case is not possible to be exported to Simulink because the Dymola block requires the compilation of the code.

In the upcoming models deriving the input signal has to be bypassed. A trivial solution is to change the configuration so that the derivation of the input is avoided. The second solution is to use a lowpass filter before the derivative block. Regarding the equation for a first order lowpass filter

$$T\dot{y} + y = Ku \quad (3.3)$$

where  $y$  is the output and  $u$  is the input, the derivation of the input is not required. Therefore, the model in figure 3.8 is compilable. The gain  $K$  has to be set equal 1 and the value of the constant  $T$  should be chosen as small as possible so that its amplitude does not change and it responds very quickly to any changes of inputs. Using the lowpass filter also ensures that the signal entering the "der()" block is continuous. The combination of both elements results in a derivative lag or DT1 element.

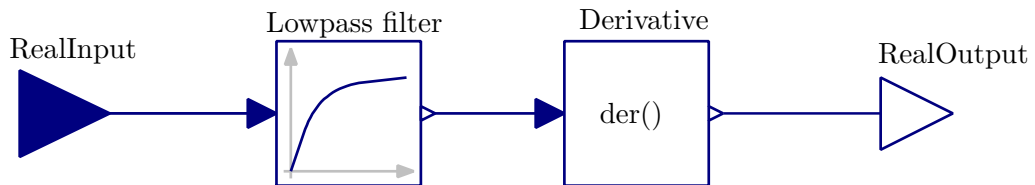


Figure 3.8: Dymola model

However, this solution works for simple models like in this example but is inapplicable for complex structured models. For every derivation of the input there has to be one lowpass filter to compensate the error. This leads to a series connection of lowpass filters which can cause instability of the output and numerical problems for the simulation. Changing the configuration is the solution in these cases. A better approach for the Dymola models in the *HumanLib* is to change the equations in a way that all incoming signals which will be derived in the model have to be filtered before. The exported versions for all three elements will be worked out in the following part.

### Exported compliance

The following part shows the equations for the compliance and it can be shown that the incoming pressure  $P_{in}$  is related to  $\Delta V$ .

$$P_{in} = C \cdot \Delta V + P_e \quad (3.4)$$

$\Delta V$  is derived in the very last equation in the compliance model.

$$\Delta \dot{V} = Q_{in} + Q_{out} \quad (3.5)$$

To avoid the derivation of  $\Delta V$  a state variable  $x$  has to be added and a low pass behavior have to be implemented. It can be shown that the variable  $x$  resembles the output of the lowpass filter. As a result, the time constant  $T_C$  is a new variable which have to be chosen as small as possible as previously explained on figure 3.8. (In addition to the new low pass filter, the algebraic sign for the outgoing flow  $Q_{out}$  has to be changed because the exported model is not part of a loop process anymore.) To realize these methods the last equation has to be changed to the following structure.

$$\dot{x} = \frac{\Delta V - x}{T_C} \quad (3.6)$$

$$\frac{\Delta V - x}{T_C} = Q_{in} + Q_{out} \quad (3.7)$$

Figure 3.9 shows the new structure for the compliance.  $P_{in}$  and  $Q_{in}$  have been chosen as input signals.

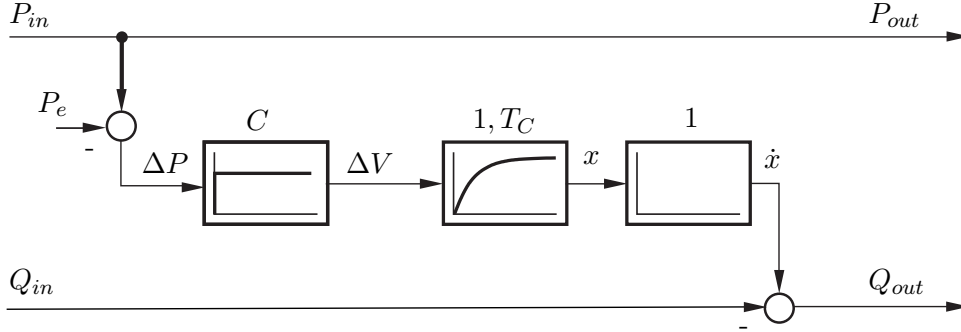


Figure 3.9: Diagram for the compliance with inputs  $P_{in}$  and  $Q_{in}$  and implemented lowpass filter

$$A_{C,export} = \begin{pmatrix} 1 & 0 \\ G_{PT1,C} \cdot C_{el} \cdot s & 1 \end{pmatrix} \quad (3.8)$$

### Exported inductance

The analog procedure executed with the compliance has to be done for the inductance as the derivation of the volume flow is needed in the model. Instead of the derivation of the incoming pressure, the incoming volume flow is derived in the model of the inductance.

$$L \cdot \dot{Q}_{in} = \Delta P \quad (3.9)$$

Same as in the previous case a low pass filter is added, so that the model can be represented by the diagram in figure 3.10. Again, the equation for the volume flow is applied to the physical

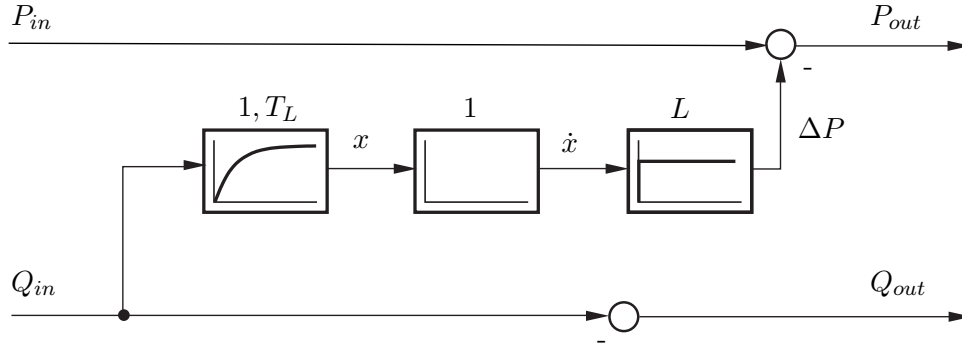


Figure 3.10: Diagram for the inductance with inputs  $P_{in}$  and  $Q_{in}$  and implemented lowpass filter

behavior in a signal oriented flow process with  $P_{in}$  and  $Q_{in}$  as inputs.

$$A_{C,export} = \begin{pmatrix} 1 & G_{PT1,L} \cdot L_{el} \cdot s \\ 0 & 1 \end{pmatrix} \quad (3.10)$$

### Exported resistance

For the resistance only the algebraic sign for the incoming flow  $Q_{in}$  has to be changed because there no input is derived in the model. Figure 3.11 shows the unmodified model of the resistance.

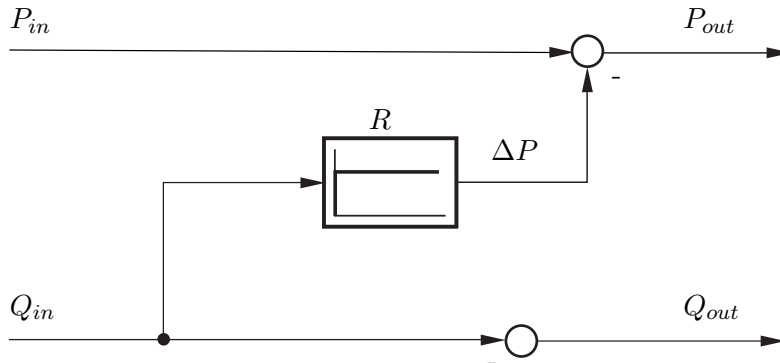


Figure 3.11: Diagram for the resistance with inputs  $P_{in}$  and  $Q_{in}$

With the three emphasized elements all configurations can be composed and exported to Simulink. The choice of inputs for the models, however, influences the structure. The following part is dedicated to this issue.

### 3.2.3 Inputs and Outputs of the Dymola Model

All Dymola objects are in interaction with the surrounding objects through the four signals,  $P_{in}$ ,  $P_{out}$ ,  $Q_{in}$  and  $Q_{out}$ .  $P_{in}$  and  $P_{out}$  are the incoming and outgoing pressure, whereas  $Q_{in}$  and  $Q_{out}$  are the incoming and outgoing volume flow. The baroreceptor and its interactions with the vessels are omitted. For every element the incoming signals are the inputs, the outgoing are the outputs. Using a simulation model, however, this configuration can be varied without changing the equations. The blocks "RealInput" and "RealOutput" are used as interfaces which import and export real discrete data.

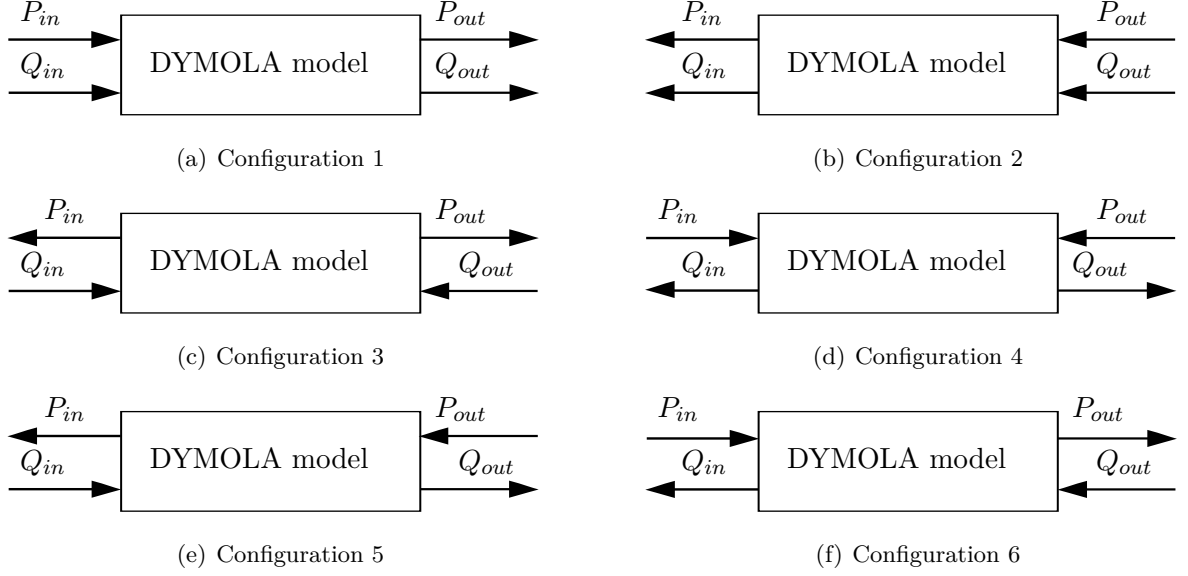


Figure 3.12: Possible configurations of inputs and outputs

To put it in a mathematical context, one can say that every element is based on two nonhomogeneous differential equations. Each equation has the structure

$$f_n(x)y^{(n)} + \dots + f_1(x)y' + f_0(x)y = g(x) + h(x) \quad (3.11)$$

$g(x)$  and  $h(x)$  are the inputs in this case. Is the signal  $y(t)$  known, so this signal can also be used as input. As all signals were measured during experiments, all possible input configurations have to be considered.

The choice of configuration highly depends on the desired calculations. The aorta is a good representing model which consists of a series connection of compliance, inertance and resistance. This is setup was already mentioned in chapter 2.5, defining the tube element. Complex models are also compounded by the three elements but in a more complex constellation. In order to understand how inputs and outputs can be chosen and what it means for the later identification, the behavior will be explained in detail with a simple model of the aorta.

#### Configurations for the aorta model

For simulations two inputs have to be predefined. Two outputs are computed by solving the equations, on which the models are based. As a result, there are six different configurations conceivable using the signals as inputs and outputs. All possible configurations are shown on

figure 3.12. These will be discussed with the model for the aorta provided by the Ursino's research as this is a simple series connection of compliance, inertance and resistance, shown as Dymola model in figure 3.13. As explained in chapter 2.5 pressure  $P$  and volume flow  $Q$  behavior can be described by using voltage  $U$  and current  $I$ . Due to this analogy a good representation

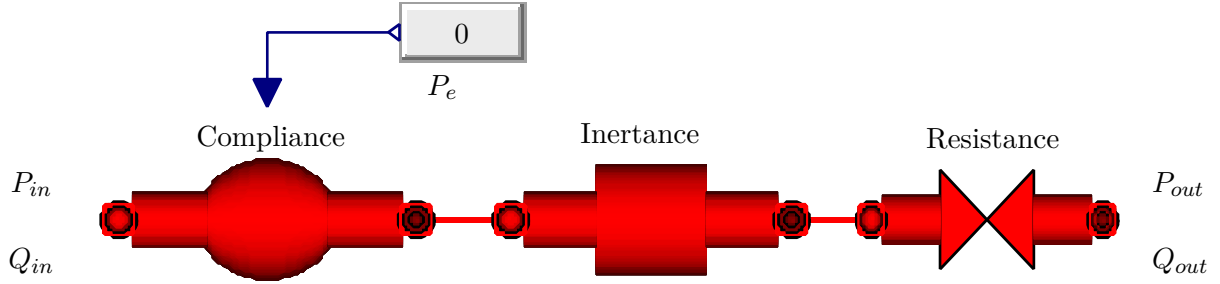


Figure 3.13: Ursino model for the aorta

is reached by using the equivalent circuit diagram for four-terminal elements which was also introduced in this chapter. For the aorta, the order changes in comparison to the setting for the elastic pipe in figure 2.11. According to the aorta model shown in figure 3.13 which is provided by the *HumanLib*, the setting from left to right is: conductor, inductor and resistor. This setting is given in figure 3.14. The value  $P_e$ , which represents the extravascular pressure on the vessel, is set to zero because there is no external force acting on the aorta according to the Ursino model.

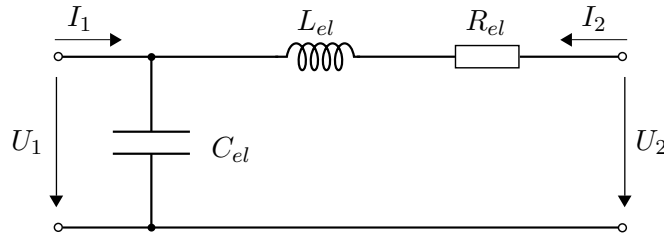


Figure 3.14: Equivalent circuit diagram for the aorta

The Kirchhoff's circuit laws reveal the relation

$$U_2 - U_1 = (R_{el} + s \cdot L_{el}) \cdot I_2 \quad (3.12)$$

$$I_1 + I_2 = s \cdot C_{el} \cdot U_1 \quad (3.13)$$

With this knowledge table is constructed showing the function diagrams of each configuration.

In the table the relation between inputs and outputs are described with a matrix and the functional diagram. The entries in the matrices show which dynamical behavior can exist. Each entry in the matrices has the structure of a transfer function

$$a_{ii} = \frac{b_m s^m + \dots + b_1 s + b_0}{a_n s^n + \dots + a_1 s + a_0}. \quad (3.14)$$

In the case that the order of the nominator  $m$  is higher than the order of the denominator  $n$  the transfer behavior is regarded as acausal and unrealizable as a real physical system. This issue is important for the export of the models from Dymola later.

For configuration 1 the signals  $U_1$  and  $I_2$  are the inputs for the model. The relationship to the outputs can be described by using a proportional block element including the resistance



value and integral block elements for both, conductance and inductance value. The functional diagram also shows that the output  $I_2$  highly correlates to the output  $U_2$ . This means that a simulation with predefined parameters computes  $U_2$  as independent signal output. For the estimation task, it means that only  $U_2$  can be fitted to the measured data.

A similar structure can be pictured for configurations 2, 3 and 4. Each configuration shows one output and one correlating signal. In configuration 2 the current  $I_1$  is the output and  $U_1$  is the integration of it. The other behavior can be taken from the table.

Configuration 5 includes PT2 behavior and, therefore, there is the danger of instability for the outputs  $U_1$  and  $I_2$ . According to the values of  $C_{el}$ ,  $L_{el}$  and  $R_{el}$ , the output does not reach a limited boundary but expands.

Configuration 6 shows that both outputs,  $U_2$  and  $I_1$ , are decoupled of each other. This means that both, either  $U_2$  or  $I_1$ , can be computed independently. The parameters for this constellation do not correlate. For the parameter estimation this means that a fitting on both outputs can be performed without the problem of interaction between the parameters. Thus, this configuration will be preferred for further calculations and used in the next chapter.

The model structure is summarized in the matrix notation for each configuration. The label for each matrix is shown underneath. According to [15] the matrices are labeled as  $A$ ,  $Z$ ,  $Y$ ,  $H$  and  $C$ . The matrix for configuration 1 has no specific name but can be described by the inverse of the  $A$  matrix.

It should be noted that only configuration 5 highlights a system which is causal and which can be exported from Dymola without problems. To avoid export errors for the chosen configuration 6, a change in the transfer behavior is necessary, which will be exposed in chapter 3.2.2.

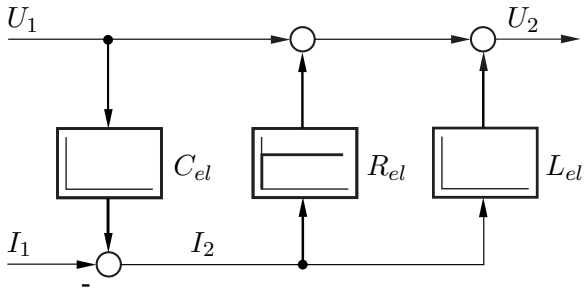
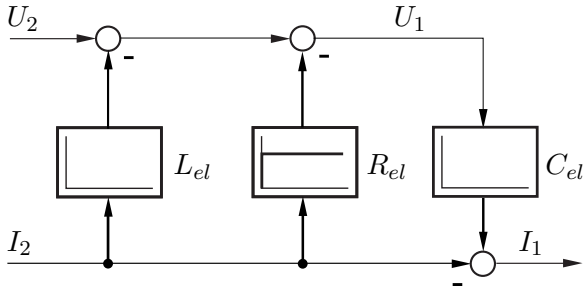
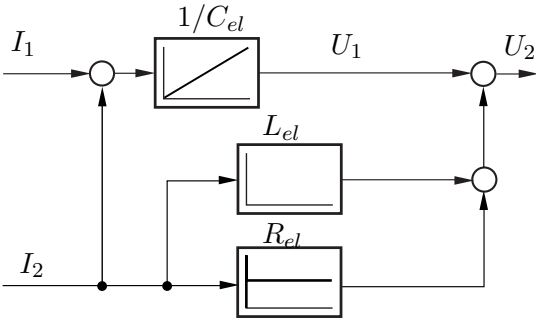
Configuration 1	$\begin{pmatrix} U_2 \\ -I_2 \end{pmatrix} = \begin{pmatrix} L_{el}C_{el}s^2 + R_{el}C_{el}s + 1 & -(R_{el} + L_{el}s) \\ -C_{el}s & 1 \end{pmatrix} \cdot \begin{pmatrix} U_1 \\ I_1 \end{pmatrix}$ 
Configuration 2	$\begin{pmatrix} U_1 \\ I_1 \end{pmatrix} = \underbrace{\begin{pmatrix} 1 & R_{el} + L_{el}s \\ C_{el}s & L_{el}C_{el}s^2 + R_{el}C_{el}s + 1 \end{pmatrix}}_A \cdot \begin{pmatrix} U_2 \\ -I_2 \end{pmatrix}$ 
Configuration 3	$\begin{pmatrix} U_1 \\ U_2 \end{pmatrix} = \underbrace{\begin{pmatrix} \frac{1}{C_{el}s} & \frac{1}{C_{el}s} \\ \frac{1}{C_{el}s} & \frac{L_{el}C_{el}s^2 + R_{el}C_{el}s + 1}{C_{el}s} \end{pmatrix}}_Z \cdot \begin{pmatrix} I_1 \\ I_2 \end{pmatrix}$ 

Table 3.3: Configurations for the aorta (I)

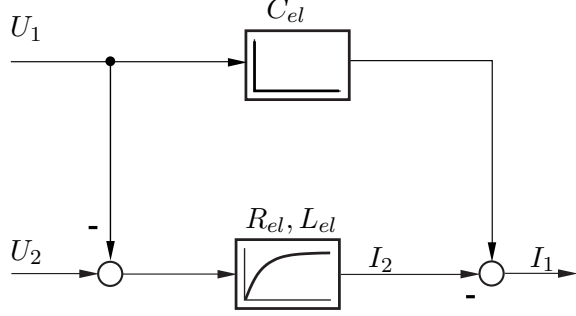
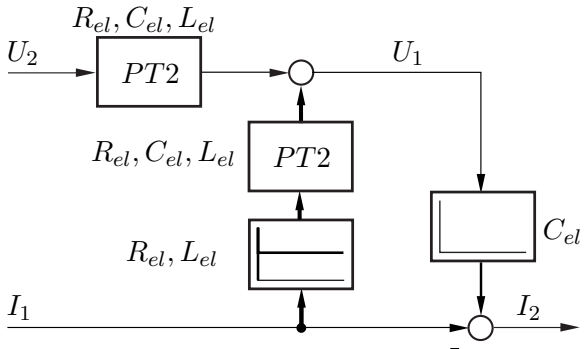
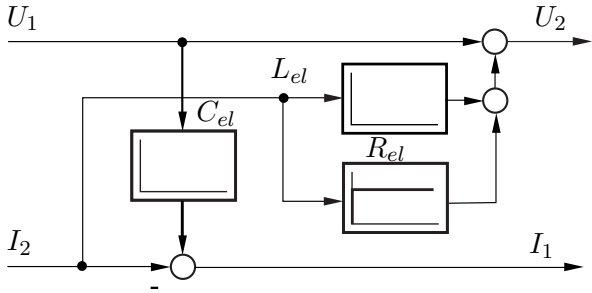
Configuration 3	$\begin{pmatrix} I_1 \\ I_2 \end{pmatrix} = \underbrace{\begin{pmatrix} \frac{L_{el}C_{el}s^2 + R_{el}C_{el}s + 1}{R_{el} + L_{el}s} & -\frac{1}{R_{el} + L_{el}s} \\ -\frac{1}{R_{el} + L_{el}s} & \frac{1}{R_{el} + L_{el}s} \end{pmatrix}}_Y \cdot \begin{pmatrix} U_1 \\ U_2 \end{pmatrix}$ 
Configuration 5	$\begin{pmatrix} U_1 \\ I_2 \end{pmatrix} = \underbrace{\begin{pmatrix} \frac{R_{el} + L_{el}s}{L_{el}C_{el}s^2 + R_{el}C_{el}s + 1} & \frac{1}{L_{el}C_{el}s^2 + R_{el}C_{el}s + 1} \\ -\frac{1}{L_{el}C_{el}s^2 + R_{el}C_{el}s + 1} & \frac{C_{el}s}{L_{el}C_{el}s^2 + R_{el}C_{el}s + 1} \end{pmatrix}}_H \cdot \begin{pmatrix} I_1 \\ U_2 \end{pmatrix}$ 
Configuration 6	$\begin{pmatrix} I_1 \\ U_2 \end{pmatrix} = \underbrace{\begin{pmatrix} C_{el}s & -1 \\ 1 & R_{el} + L_{el}s \end{pmatrix}}_C \cdot \begin{pmatrix} U_1 \\ I_2 \end{pmatrix}$ 

Table 3.4: Configurations for the aorta (II)

### Configurations for more complex models

The model structure for a vessel is clearly and an analysis of all configurations can be carried out. For more complex models such as the pulmonary or the systemic circulation the number of elements is high so that a graphical representation with functional diagrams does not provide a good overview. Therefore, configurations for these models will be regarded with the matrix representation. Every system can be composed by a matrix product of all including elements. For series connections there is

$$\begin{pmatrix} U_1 \\ I_1 \end{pmatrix} = \underbrace{\prod A_i}_{A_{result}} \cdot \begin{pmatrix} U_2 \\ -I_2 \end{pmatrix} \quad (3.15)$$

As a result the matrix  $A_{result}$  describes the behavior of the composed system. The order of each element in the system has to be preserved in the matrix product and changes in the order can lead to a different structure. The matrix  $A_{result}$  is analyzed by transforming it into the other matrices  $Z$ ,  $Y$ ,  $H$  and  $C$ . For complex models the task is to find the configurations which feature a causal transmission behavior between the inputs and outputs. The initially mentioned approach to solve the export error from Dymola can easily be avoided and the lowpass filters are not necessary for these configurations.

The circuit diagram for the pulmonary circulation is shown in 3.15. For this representation all external pressure effects on the pulmonary vessels are not considered and, therefore, assumed to be zero. Thus, all including conductors can be regarded as grounded. This assumption is a clear reduction of the system and differs to the model considerations in the *HumanLib*. For the estimation of parameters, mostly data for a short time interval can be used due to the strict boundaries (see next chapter). In this interval the external pressure change is irrelevant and, therefore, the reduction can be applied with good approximation to the actual model. However, for other tasks the influence of external pressure has to be considered in the electric circuits, too. This can be done by including active elements such as energy sources. Further studies about this considerations will be part of chapter 4.

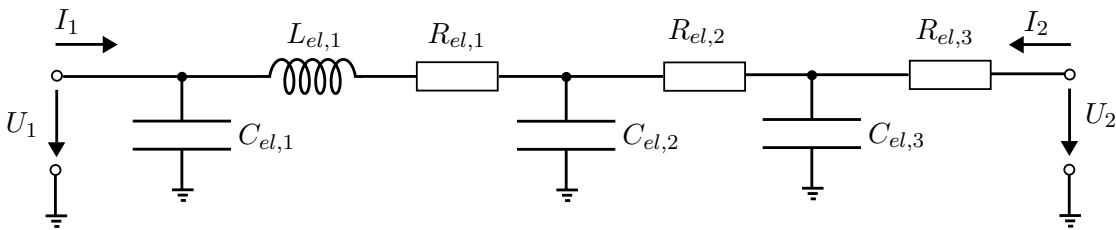


Figure 3.15: Circuit diagram for the pulmonary circulation

With Matlab functions the matrix product for  $A_{result}$  and the transformations can be computed. The test for causality also can be executed by comparing the order of numerator and denominator for the variable  $s$ . As a result the matrices  $Z$  and  $H$  determine the configuration in which the system is causal. Considering table that means that either both currents are determined as inputs or  $I_1$  and  $U_2$ . With these preliminary considerations the parameter estimation can be carried out in the way it was exposed in chapter 2.

### 3.3 Estimation Procedure and Results for Parameters

In this section the presented models will undergo a parameter estimation in Simulink. The preprocessed data is shown in figure 3.16. All signals were filtered by applying FIR filters and resemble a better physical behavior than the measured.

For the estimation the data is divided into training and validation data. The training data is compared to the model output during the estimation processes and helps to find the right setting for the parameters so that the measured data fits to the simulated. With the validation data the quality of the model is evaluated. For that reason, the resulting computed model output is compared to the measured data, which was chosen as validation set. With the validation step the accuracy of the model to the real system is checked. However, for the given task, the measured data is superimposed with noise and the accuracy to the real system output is unsatisfactory. A validation can be omitted at this point.

LVP and LVQ will be set as the inputs for the aorta and AoP and AoQ as the outputs. The outputs are measured in the aorta itself and, therefore, this setting leads to an estimation for the ascending aorta and parts of the aortic valve. This segment starts in the left ventricle and leads to the point where the sensor for AoP and AoQ was applied. This assumption is acceptable at this point because the estimation task in this thesis focuses on the compatibility of measured data and models. Another better setting will on the left side the progresses for both pressures are plotted. On the right side the volume flow is shown. The lines in red color stand for the ventricular quantities, LVP and LVQ. The black lines are the aortic measured signals, AoP and AoQ.

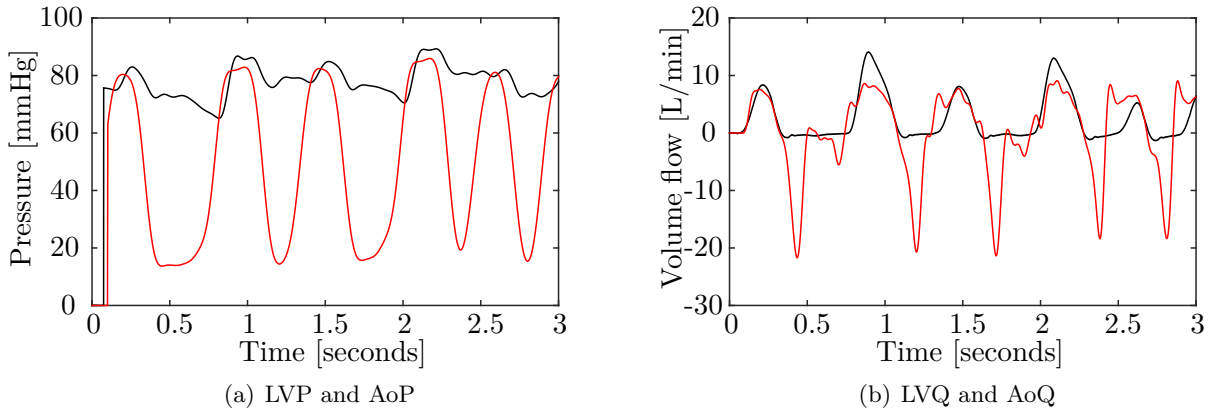


Figure 3.16: Preprocessed input and output signals

For the estimation of parameters in the aorta, it has be ensured that the flow stream through the aorta is directed to the systemic circulation and the pressure at the entrance is higher than at the end. This state is given when the absolute differences  $\Delta P_{aorta}$  and  $\Delta Q_{aorta}$  are both positive:

$$\Delta P_{aorta} = LVP - AoP \quad (3.16)$$

$$\Delta Q_{aorta} = LVQ - AoQ \quad (3.17)$$

This constraints are fulfilled between 2.57 and 2.61 seconds. The absolute differences of pressure and volume flow are plotted in figure 3.17.

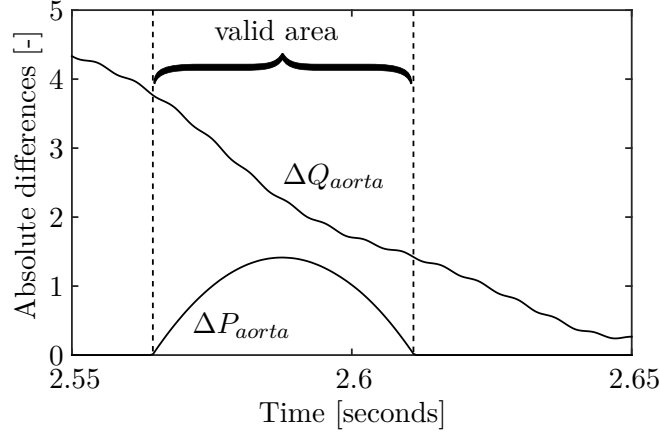


Figure 3.17:  $\Delta P_{aorta}$  and  $\Delta Q_{aorta}$

The curly bracket marks the valid area which satisfy the requirements. The including data set will be used as input and output data.

### 3.3.1 Parameter estimation for the aorta

For the aorta the Dymola model in figure 3.13 based on Ursino's research is used for the estimation procedure. The compliance, resistance and inertance of the aorta will be chosen to be estimated. The inputs for the model will be chosen according to configuration 6 because both outputs, the three parameters  $C$ ,  $R$  and  $L$ , are decoupled, as explained in the earlier section. This assures that both outputs can be fit to measured data without interacting with the other. So, all measured information can be used for the estimation and a preciser identification of the parameters can be executed.

First, the Dymola model is adjusted to the configuration with  $P_{out}$  and  $Q_{in}$  as inputs.

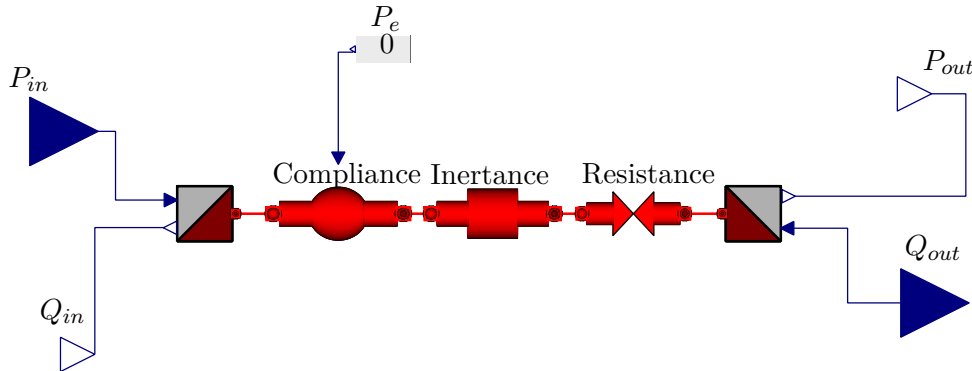


Figure 3.18: Dymola model for aorta with configuration 6

This model is compiled and exported to Simulink and connected to import and output blocks. The export model is shown in figure 3.19 on the left. In addition to that, the physical structure of inputs and outputs is given as functional diagram on the left. In comparison to the diagram of configuration 6 in table 3.4, PT1 elements are added to avoid the described export error.

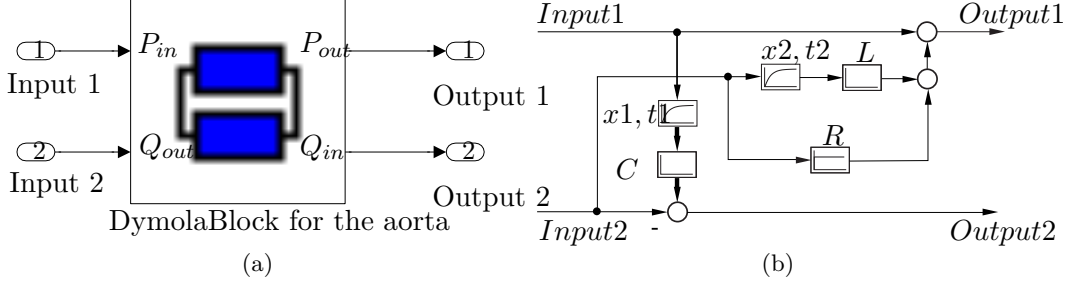


Figure 3.19: Export model for aorta in Simulink

Input 1 is linked with LVP and input 2 with AoQ. Output 1 is compared with AoP, while output 2 with LVQ.

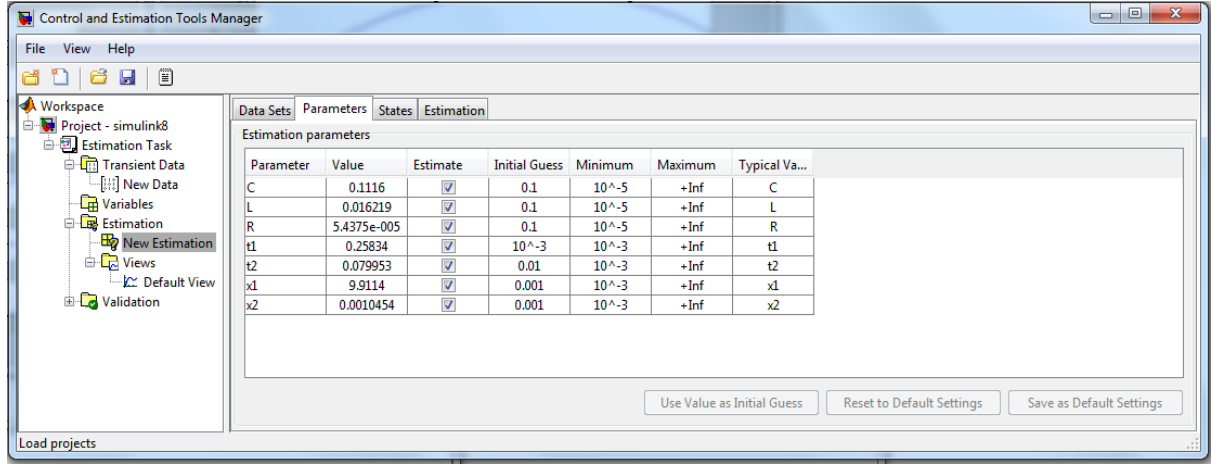


Figure 3.20: Chosen parameters for the estimation task

The following parameters are chosen to be estimated:  $C$ ,  $L$ ,  $R$ ,  $t1$ ,  $t2$ ,  $x1$  and  $x2$ . Figure 3.20 shows the window with the selection and their boundaries.  $t1$ ,  $t2$ ,  $x1$  and  $x2$  are the parameters for the PT1 elements. While  $t1$  and  $t2$  are the time parameters,  $x1$  and  $x2$  are the start value for the outgoing signal.

The physical boundaries for the parameters is that no value becomes negative. That is why the minimum value is set to  $10^{-3}$  for  $C$ ,  $L$  and  $R$  and  $10^{-5}$  for the others. The upper boundary for all parameters is open. The initial guess for each value is chosen randomly to a values, which are close to the expected parameters for the human body.

The setting for simulation and optimization is shown in figure 3.21. For simulations the variable-step solver ode45 (Dormand-Prince) is used, because it promises the best order of accuracy in comparison to the other possible solvers. The optimization method is based on nonlinear least squares and the Levenberg-Marquadt algorithm. The simulation time is determined to 91 steps as there is a data set of this number of measured data points chosen as input. The zero crossing control is switched on. This function avoids that the solver sets time steps excessively small in case of discontinuities. The run time is improved by this option.

All settings concerning the step size are set to be controlled automatically and will be computed by the solver. All fields listed under *Optimization options* can be chosen according to the

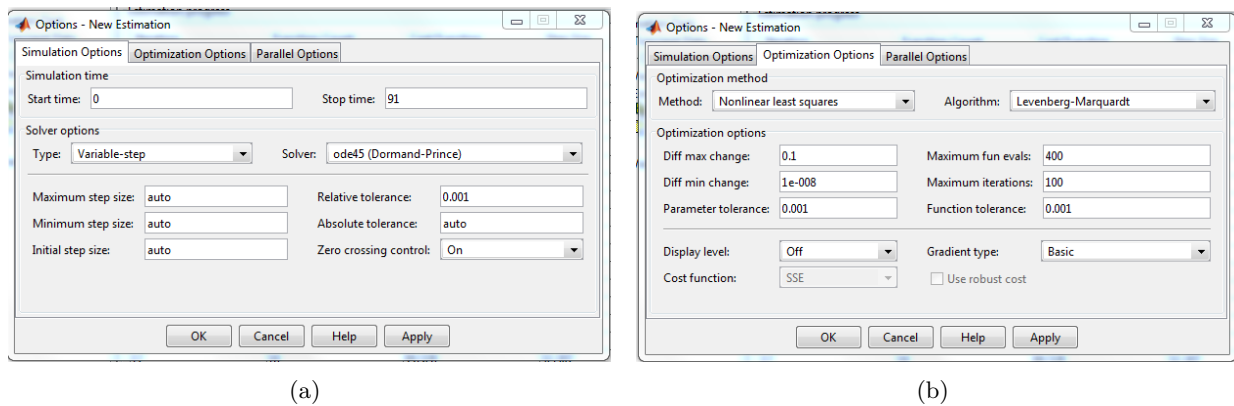


Figure 3.21: Setting for simulation and optimization

desired termination condition for the iterations. On the one hand the boundaries for maximal and minimal changes of parameters or parameter tolerances can be predefined. On the other hand, the maximum number of function evaluations or maximum iterations can be set. The last option provides the option to limit the function tolerance.



Using this setting results in an estimation progress with 14 iteration steps, shown in figure 3.22. For each step the value of the cost function declines and approaches asymptotically to a value of 671. On the other hand, the step size varies. The iteration process stops because the function tolerance reached a value of  $2 \cdot 10^{-4}$  in the last iteration step, which is less than the limit value of 0.001. This value was predefined in the window for optimization setting, shown in figure 3.21. The function count increases by one per each step which means that there is one cost function which is calculated each time.

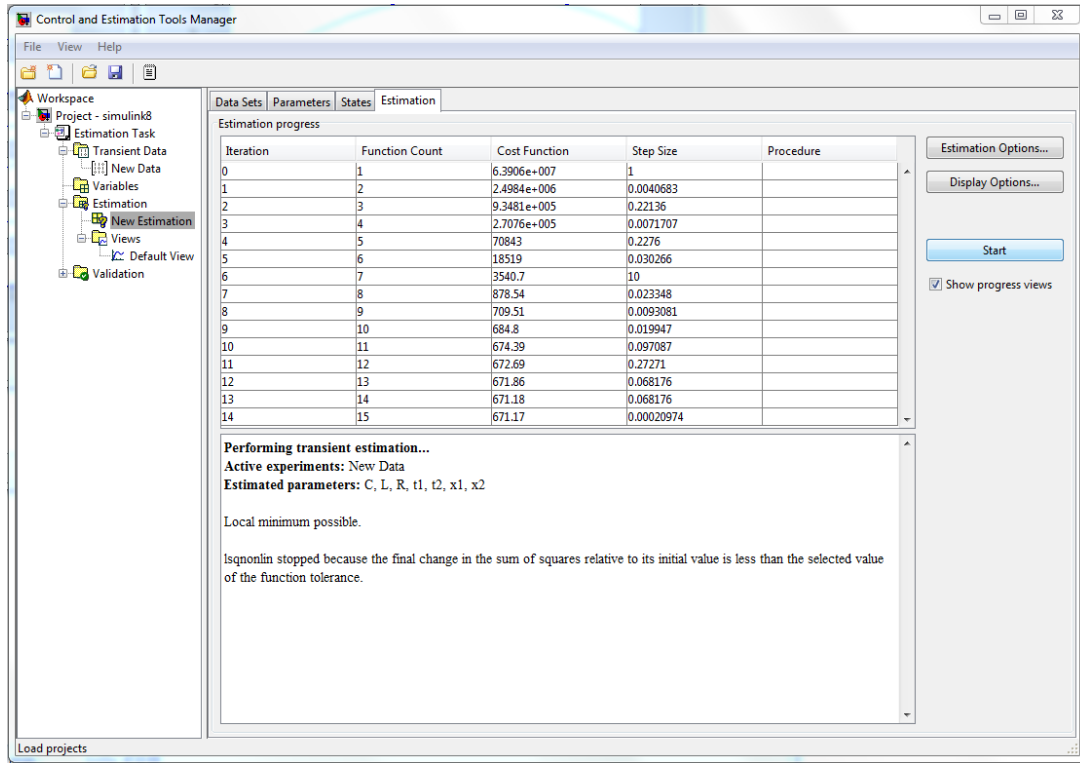


Figure 3.22: Estimation progress

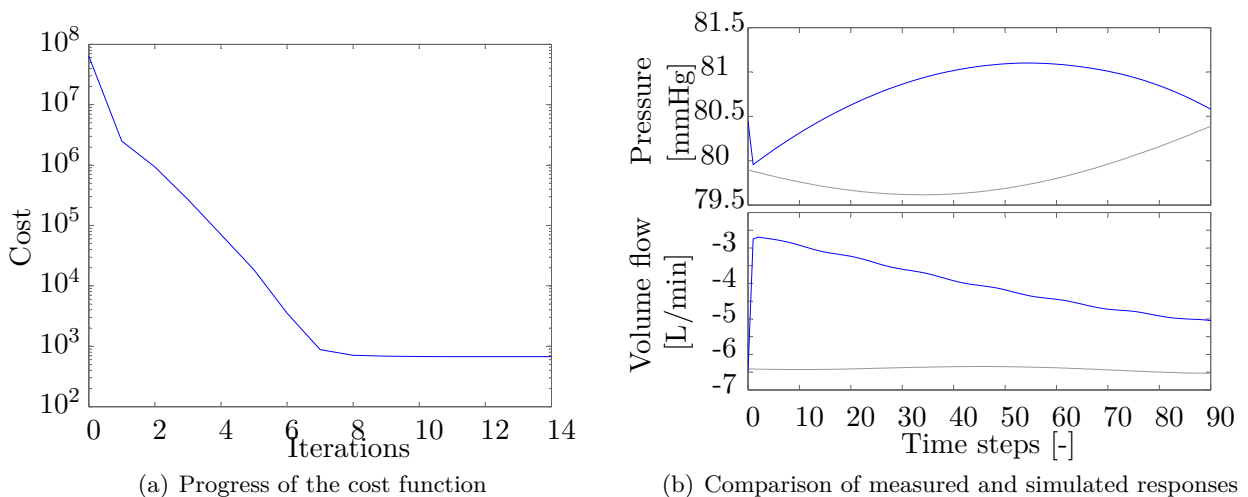


Figure 3.23: Cost function and outputs

The progress for the cost function is plotted in figure 3.23 (a). As already mentioned, it steady decreases. The comparison of the measured signals AoP and LVQ against the simulated response of the model is shown in 3.23 (b). The blue lines indicate the simulated signals. The volume flow is negative because it was defined as an outgoing signal. The parameters are computed in each step. The trajectories of estimated parameters can be found in figure 3.24.

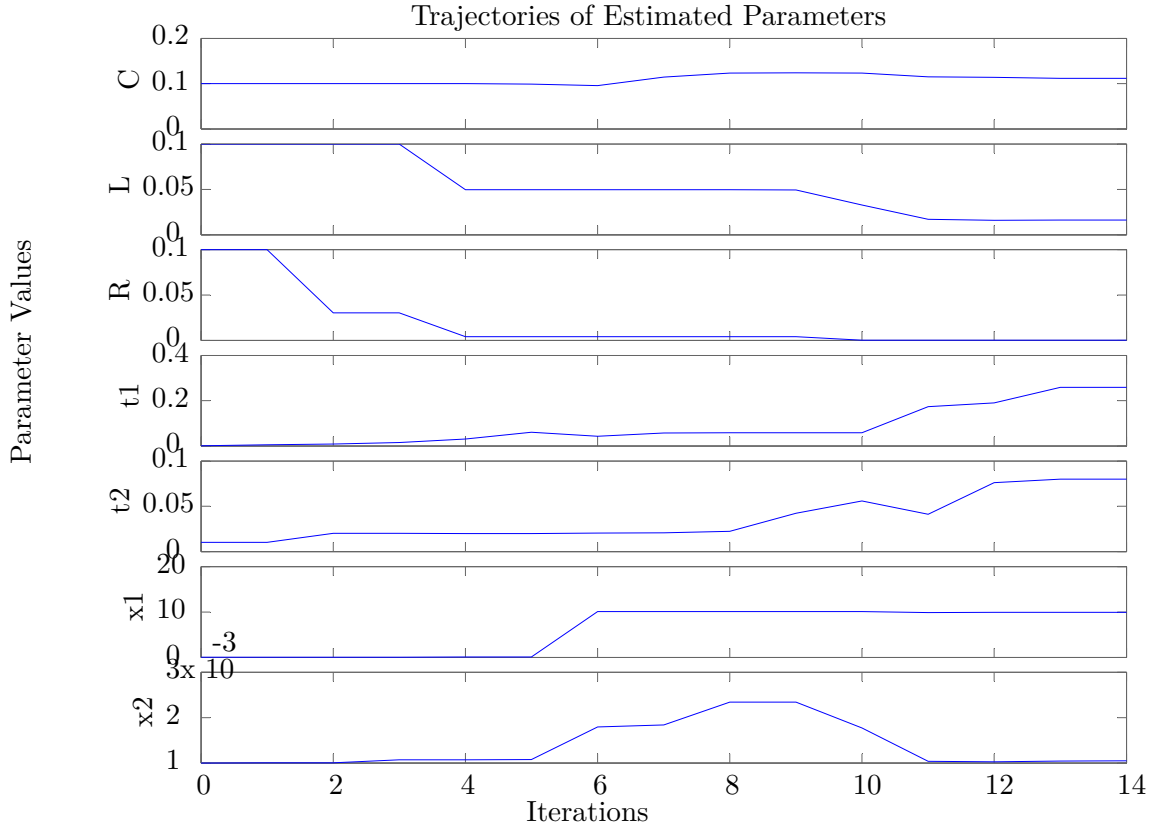


Figure 3.24: Progress for parameters

All parameters vary during the estimation and reach a final value in iteration step 14. The final value can be found in figure 3.20.  $t_1$  and  $t_2$  are relatively small with values of about 0.26 and 0.08 in comparison to the complete simulation time of 91 steps. Therefore, the PT1 element's dynamics can only be detected at the very beginning of the simulation. In figure 3.23 the progresses of the outputs indicate a jump, which can be traced back to the dynamic effect. The derived system structure in figure 3.19 (b) is verified by a parameter estimation without the parameters  $C$ ,  $x_1$  and  $t_1$ . In that case the volume flow can not be affected by varying the remaining parameters. This case transferred to the functional diagram means that the branch with the PT1 element including parameters  $x_1$  and  $t_1$  and the followed derivative block would miss. Output2 is equal to the negative signal of Input2 and cannot be changed by any variation in the model. Therefore, the system structure matches.

---

## Statistical Study and Sensitivity Analysis

---

In earlier research papers about cardiovascular systems models of vessels, as used in chapter 3, were built up and used for simulations of the pressure and volume flow in the human body. With a combination of these partial models to a circulation system the whole body can be modeled. In systems as complex as the body, the relevances of consisting components and its effect on the outputs is unknown. In order to give good predictions with complex models for cardiovascular purposes, a critical controversy about the output quality is necessary. An analysis about the sensitivity of factors helps to identify the influence of the components and factors on the quality of the model output and to improve the model structure with the gained knowledge. In context with biological processes a good definition of sensitivity is given by Nestorov: a sensitivity analysis is "the systematic investigation of the model responses to either i) perturbations of the model quantitative factors (e.g. inputs and/or parameters) or ii) variations in the model qualitative factors (e.g. structure, connectivity modules or submodels)" [9].

For mathematical models most works focus on the investigation of quantitative factors such as the including parameters. Especially, complex systems contain large numbers of parameters, whose values and importance to the model are in question. The result of the analysis in this chapter is to highlight and use methods which identify the parameter significance.

There are two common ways to analyze sensitivity. On the one hand, there is the global sensitivity analysis, in which the parameters are varied over their full domain of definition and the effect on the behavior is assessed. Alternatively, a local sensitivity analysis can be applied. In this method the behavior of a chosen output is computed for a small variation of one parameter around a fixed point. This task leads to a differentiation of a chosen output with respect to one or more parameters, described in 2.6. The focus in the following section will be a local sensitivity analysis.

## 4.1 Local sensitivity analysis for parameters

For an investigation in terms of a sensitivity analysis an output has to be chosen first. In case of the model structure shown in figure 3.14 possible outputs are one of the currents  $I_1$  or  $I_2$ , or the voltages  $U_1$  or  $U_2$ . By solving the model equations, a time and parameter dependent function for the output is computed. If this function is derivable, it can be derived with respect to one or more parameters to compute the local sensitivity. The resulting derivatives are identical to the coefficients of the sensitivity matrix  $Z$  introduced in 2.6. By comparison of all coefficients, a qualitative statement about the importance of each parameter is possible.

A way for local sensitivity analysis is to use Laplace transformation in order to solve the ODE. Applying this, once for the basic setting and another time with an incremented value for the parameter, results in two solutions for the output. With equation 2.15 the sensitivity can be computed easily by dividing the difference of both solutions by the difference of the initial and incremented parameter value. To do so, outputs and parameters have to be predefined. In this chapter the outgoing current  $i_2(t)$  is chosen and investigated. All input signals are arbitrarily in the following considerations, so that this part of the thesis can be regarded as a thought experiment.

The explained algorithm will be elaborated for the model of the aorta and the pulmonary circulation.

### 4.1.1 Sensitivity of the aorta

For the aorta model the sensitivity of the parameters  $C$ ,  $L$  and  $R$  define how the behavior of the model reacts. If one of these parameter changes its value, the effect on the outgoing current  $i_2(t)$  has to be examined. Apart from these factors, the influence of external pressures on the vessel is in question. Although the aorta is not applied with any external pressure according to Ursino's assumptions, an investigation on it reveals insights for further studies on other types of vessels and on models of more complex structures.

Contrary to former assumptions in this thesis, the transmural pressure will be respected now, which means that the compliance structure introduced in chapter 3.2.1 has to be changed. The new element is shown in figure 4.1 (a) and can be considered as an extension for figure 3.2. The

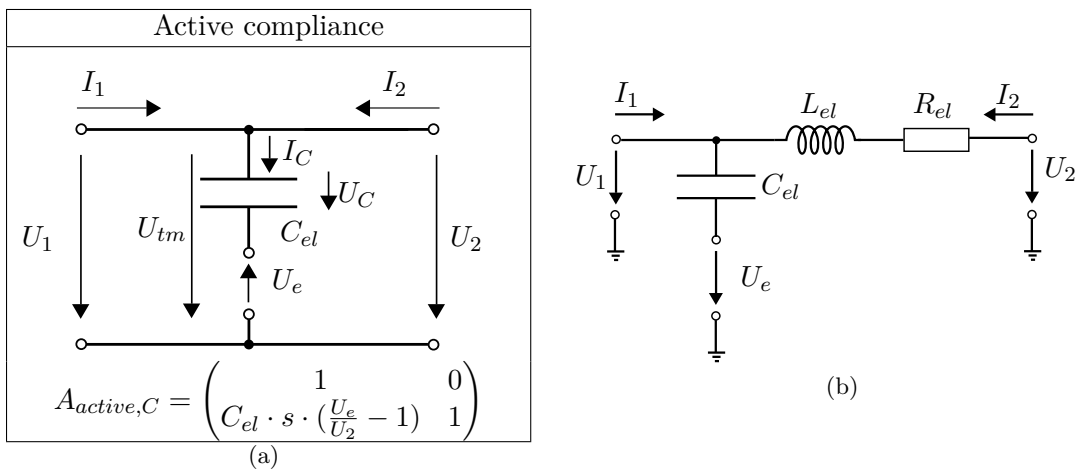


Figure 4.1: Extended aorta model

matrix for the active compliance element contains the voltage  $U_e$ , which resembles the external pressure  $P_e$ . The entries for the matrix  $A_{active,C}$  results from a combination of the voltage source  $U_e$  and the conductor with  $C_{el}$ . The entry for the matrix is derived by the following

calculation:

It is

$$C_{el} \cdot s \cdot U_C = I_C \quad \text{and} \quad U_{tm} = U_C - U_e \quad (4.1)$$

As a result, the equation for the current is

$$C_{el} \cdot s \cdot (U_{tm} + U_e) = I_C \quad (4.2)$$

$$\Rightarrow C_{el} \cdot s \cdot (-U_2 + U_e) = I_C \quad (4.3)$$

$$\Rightarrow C_{el} \cdot s \cdot \left(\frac{U_e}{U_2} - 1\right) \cdot U_2 = I_C \quad (4.4)$$

The Kirchhoff's circuit laws for current

$$I_1 + I_2 = I_C \quad (4.5)$$

must be fulfilled. Therefore, the equation 4.4 can be found as the coefficient in the first column and second row of the matrix  $A_{active,C}$ . With this consideration, the circuit diagram for the aorta model looks like figure 4.1 (b). The local sensitivity analysis will be applied on this model. The model equations are again computed by the matrix product of the three elements, but this time the active compliance is used instead of the passive one. The equations are:

$$\begin{pmatrix} U_1 \\ I_1 \end{pmatrix} = A_{active,C} \cdot A_L \cdot A_R \cdot \begin{pmatrix} U_2 \\ -I_2 \end{pmatrix} \quad (4.6)$$

$$\Rightarrow U_1 = U_2 - I_2 (R_{el} + L_{el} s) \quad (4.7)$$

$$\Rightarrow I_1 = C_{el} s U_2 \left(\frac{U_e}{U_2} - 1\right) - I_2 \left(C_{el} L_{el} \left(\frac{U_e}{U_2} - 1\right) s^2 + C_{el} R_{el} \left(\frac{U_e}{U_2} - 1\right) s + 1\right) \quad (4.8)$$

One of the equations 4.7 or 4.8 can be used for the computation of a desired output.

### Example

The current  $I_2$ , which corresponds to the outgoing flow, will be regarded in the following. After transposing equation 4.7, it is

$$I_2 = \frac{\frac{\Delta U}{L_{el}}}{s + \frac{R_{el}}{L_{el}}} \quad \text{with} \quad \Delta U = U_2 - U_1 \quad (4.9)$$

The inverse Laplace transform can be applied to get the time dependent function of  $I_2$ . The local sensitivity analysis is performed by deriving the time dependent function with respect to its parameters. First, the including parameters and the signal  $\Delta U$  has to be predefined. Assuming the voltage difference  $\Delta U$  as constant over time with value  $K$  and zero for the time before ( $t < 0$ ), the signal can be regarded as a step function. The Laplace transformation for the function can be found in standard tables.

$$\Delta U(t) = K \quad \circ \text{---} \bullet \quad \Delta U = \frac{K}{s} \quad (4.10)$$

Following parameters occur in the model equation:

$$K, \quad L_{el}, \quad R_{el}, \quad C_{el}. \quad (4.11)$$

The inverse Laplace transform results in the following relation

$$I_2 = \frac{\frac{K}{L_{el}}}{s^2 + \frac{R_{el}}{L_{el}} \cdot s} \quad \bullet \text{---} \circ \quad i_2(t) = \frac{K}{L_{el}} \cdot (1 - e^{-\frac{R_{el}}{L_{el}} t}) \quad (4.12)$$

while  $i(t)$  is the time depended function for the current in the circuit. It can be regarded as the unit step response of a PT1 element. Therefore, an exponential function is expected. As  $i(t)$  is steady and differentiable for all parameters:

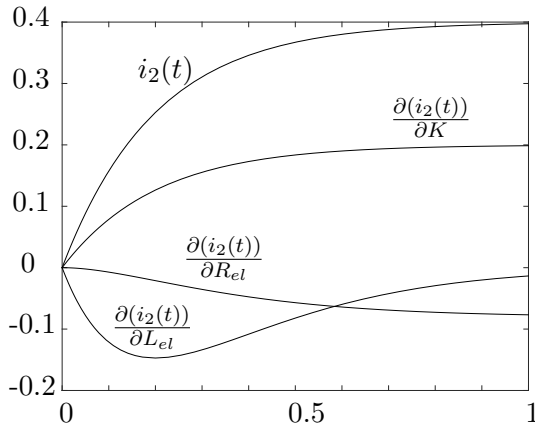
$$\frac{\partial(i_2(t))}{\partial K} = \frac{1}{L_{el}} \cdot (1 - e^{-\frac{R_{el} \cdot t}{L_{el}}}) \quad (4.13)$$

$$\frac{\partial(i_2(t))}{\partial L_{el}} = \frac{K}{L_{el}^2} \cdot (e^{-\frac{R_{el} \cdot t}{L_{el}}} - 1) - \frac{K R_{el} \cdot t}{L_{el}^3} \cdot e^{-\frac{R_{el} \cdot t}{L_{el}}} \quad (4.14)$$

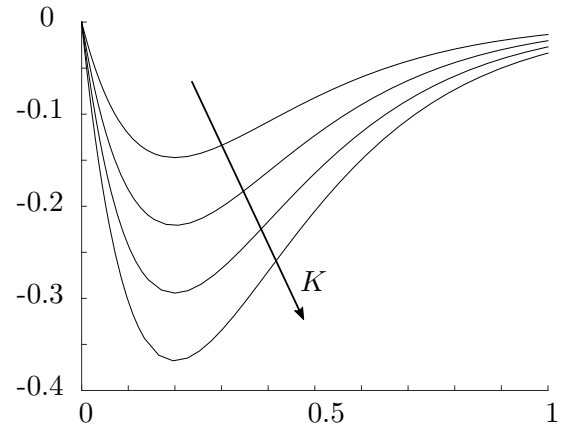
$$\frac{\partial(i_2(t))}{\partial R_{el}} = \frac{K \cdot t}{L_{el}^2} \cdot e^{-\frac{R_{el} \cdot t}{L_{el}}} \quad (4.15)$$

$$\frac{\partial(i_2(t))}{\partial C_{el}} = 0 \quad (4.16)$$

Fixed freely chosen values for  $K$ ,  $L_{el}$ ,  $R_{el}$  and  $C_{el}$  evolve the plotted function in figure 4.2 (a). The progress and behavior is focused and, thus, the actual values of the parameters are not notable. For the case that time tends to infinity, all equations approximate a final fixed value.



(a) Plotting for  $i_2(t)$ ,  $\frac{\partial(i_2(t))}{\partial K}$ ,  $\frac{\partial(i_2(t))}{\partial L_{el}}$ ,  $\frac{\partial(i_2(t))}{\partial R_{el}}$



(b) Plotting of  $\frac{\partial(i_2(t))}{\partial L_{el}}$  for a different values for  $K$

Figure 4.2: Parameter sensitivity for the aorta

This case resembles the volume flow for a predefined constant pressure difference. One can see that the function  $i_2(t)$  rises exponentially to a value of 0.4. The sensitivity of the inductance  $\frac{\partial(i_2(t))}{\partial L_{el}}$  features a remarkable progress during the transition. It steadily decreases until it reaches a minimum at about 0.2 seconds. After that it approximates to zero again. In combination with the current, it exactly represents the functionality of an inductor, which resists the change of a current. When the current is constant, the inductor has no influence on the current progress anymore.

In addition to that computation, a stepwise variation of  $\Delta U$  was done and the sensitivity for the inductance  $\frac{\partial(i_2(t))}{\partial L_{el}}$  is plotted for this variation in 4.2 (b). The increase of  $K$  means that the current progress will increase steeper for the same setting of parameters. The inductance sensitivity will decrease with the steeper slope of  $i_2(t)$ . In figure 4.2 (b) this phenomena can be indicated by a decline of the function values for each step of  $K$ . It can be stated that the compliance for this input setting has no impact on the progress of  $i_2(t)$  ( $\frac{\partial(i_2(t))}{\partial C_{el}} = 0$ ).

### Sensitivity of Ursino's aorta

In the next step the influence of the external pressure and the aortic parameters will be considered. For this investigation equation 4.8 is used. In comparison to the previous example, the parameters for the model will be taken from Ursino's approach [2] and another input setting will be used. The parameters are:

$$C_{el} = 0.28, \quad L_{el} = 0.00022 \quad \text{and} \quad R_{el} = 0.06 \quad (4.17)$$

The function for the current  $I_2$  is

$$I_2 = f(U_e, U_2, I_1) \quad (4.18)$$

$U_e$ ,  $U_2$  and  $I_1$  are considered as inputs in the Laplace plane. The sensitivity for all relevant parameters can be computed for different progresses of  $U_2$  and  $I_1$ . In this experiment  $U_2$  is considered as constant and  $I_1$  is variable in time. The variability will be expressed with a sinus function. Furthermore, the values for the quantities will be set approximate to the real the behavior in the aorta.

The approximation for the partial derivative  $\frac{\partial i_2(t, p_i)}{\partial p}$  with respect to a parameter  $p$  will be reached by the assumption:

$$\frac{\partial i_2(t, p)}{\partial p} \approx \frac{\Delta i_2(t, p)}{\Delta p} = \frac{i_2(t, p) - i_2(t, \epsilon \cdot p)}{p - \epsilon \cdot p} \quad (4.19)$$

The signals are defined in the time domain as

$$u_2(t) = 70 \quad (4.20)$$

$$i_1(t) = \frac{5}{2} \sqrt{2} \sin(\sqrt{2} t) + 10 \quad (4.21)$$

$$u_e(t) = U_e = 100 \quad (4.22)$$

$$\epsilon = 1 + 10^{-3} \quad (4.23)$$

As  $u_e(t)$  is considered to be constant, it can be equally treated as the parameters. For a variation of  $C_{el}$ ,  $R_{el}$ ,  $L_{el}$  and  $U_e$ , equation 4.19 is applied. The progress of  $i_2(t)$  is plotted in figure 4.3 the sensitivity for all parameters in figure 4.6. Due to the oscillation of  $i_1(t)$  and

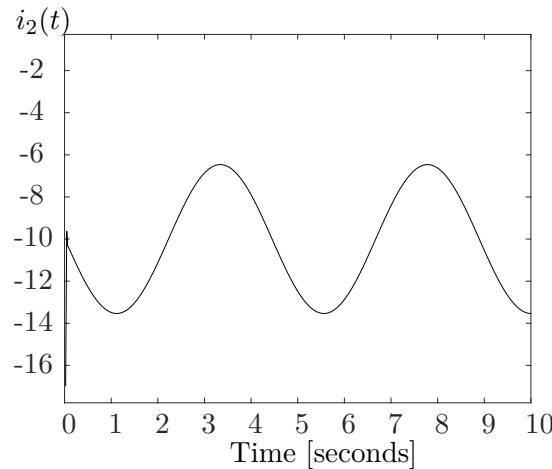


Figure 4.3: Resulting progress of  $i_2(t)$

the constant pressures, the outgoing current  $i_2(t)$  also performs an harmonic oscillation. The

shown sensitivities are the derivation of the signal  $i_2(t)$  with respect to the four parameters and, therefore, show a similar oscillation behavior. The maximums and minimums can be interpreted as the location where the parameter has its maximal influence on the current  $i_2$  in the chosen time interval. On the other hand the zero-crossings indicate the locations where the parameter has no influence locally.

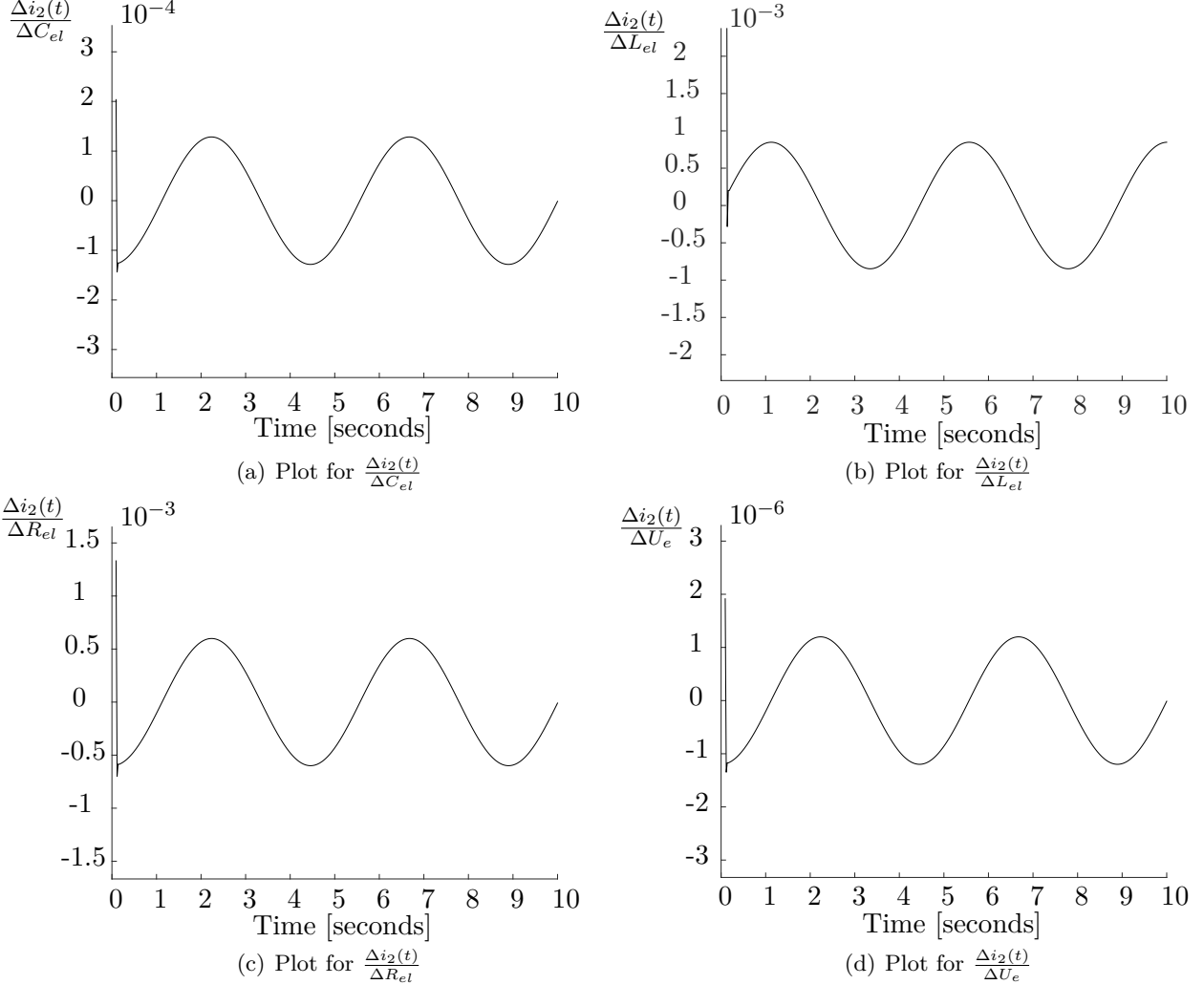


Figure 4.4: Sensitivities for  $C_{el}$ ,  $L_{el}$ ,  $R_{el}$  and  $U_e$

The sensitivities show a transient area indicated by the unsteady progress during the very first seconds.

By comparing the dimension of the amplitudes it can be stated that the relative variation of  $10^{-3}$  for the inductance  $L_{el}$  and the resistance  $R_{el}$  has the higher influence on  $i_2(t)$  in the chosen operating point than the others. The sensitivity of the external voltage  $U_e$  has the lowest dimension. For the aorta itself, this conclusion corroborates the fact that  $U_e$  is neglected in Ursino's approach. However, any other kind of vessel model in the *HumanLib* has the same structure. For a good model quality a sensitivity analysis helps to define model structures, which resemble the physical reality of each vessel.

The procedure was elaborated on the aorta to focus on the methods for the sensitivity analysis itself. In a next step the pulmonary circulation is regarded in a more relevant context.



## 4.2 Sensitivity of the pulmonary circulation

The elaborated methods can also be carried out with more complex systems such as the pulmonary circulation. Different to the aorta, this system is applied with a variable external pressure according to Ursino. The dimension of the influence is expected to be visible and comparable to the influence which any other relevant parameter has on the system. With the considerations pictured in figure 4.1, the full structure of the pulmonary circulation is shown in 4.5. Again, the matrix multiplication for this structure is performed.

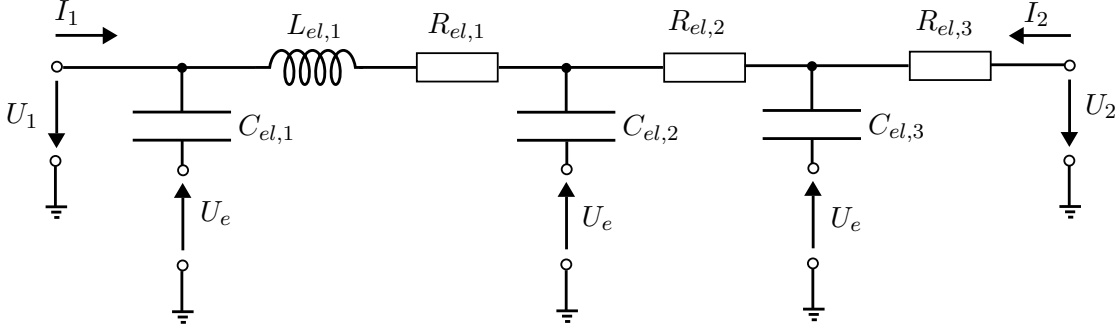


Figure 4.5: Circuit diagram for the pulmonary circulation

As a result, the function for the outgoing current depends on the variable signals  $u_e(t)$ ,  $u_1(t)$  and  $u_2(t)$ .

$$I_2 = f(U_e, U_1, U_2) \quad (4.24)$$

$$u_1(t) = \frac{5\sqrt{2}\sin(\sqrt{2}t)}{2} + 15 \quad (4.25)$$

$$u_2(t) = 5 \quad (4.26)$$

$$u_e(t) = 40 \quad (4.27)$$

$$\epsilon = 1 + 10^{-3} \quad (4.28)$$

The results of the computation for the sensitivities is shown in figure 4.6. As the transient oscillation is irrelevant, the highlighted time frame starts at second 10 and endures until second 30. Both, the sensitivity of  $i_2$  to the external pressure and to the resistance  $R_{el,3}$  are plotted in figure 4.6 (b). Comparing them with each other shows that the dimension differ. The amplitudes and domain for the external pressure is lower. This means that the influence of this parameter at the chosen operating point is unexpectedly low. Therefore, for the modeling the importance of the external pressure, as it is considered by Ursino, has to be questioned.

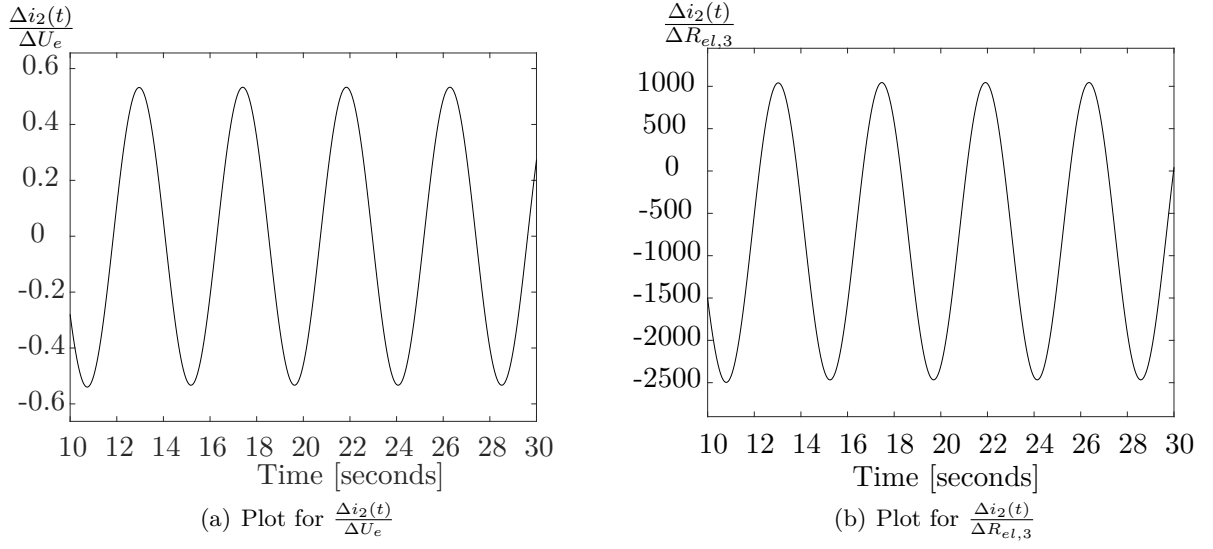


Figure 4.6: Local sensitivities for the pulmonary circulation

#### 4.2.1 Fast sensitivity analysis with matrix representation

A fast analysis of sensitivity without solving the differential equations of the system can be achieved by deriving the matrices for all configurations. For the aorta model all matrices have been computed and are shown in table 3.4. For the A matrix, for example, the computation is

$$\frac{\partial}{\partial p} \begin{pmatrix} U_1 \\ I_1 \end{pmatrix} = \frac{\partial}{\partial p} (A) \cdot \begin{pmatrix} U_2 \\ -I_2 \end{pmatrix} \quad (4.29)$$

while  $p$  can be assumed as any parameter, which is included in the matrix. This way provides a faster approach, which can be easy to implement as a function.

---

## Discussion

---

The combination of measured data and computer model is the key issue in this thesis. As a possible approach, a parameter estimation was carried out (chapter 3), whose results will be discussed in the following. In addition to that, a matrix representation including the system structure was introduced and helped to understand the behavior of outputs and inputs. In combination with a sensitivity analysis, the relevance of chosen including parameters was questioned (chapter 4). A study about a closed loop model will show what possibilities and limits the system representation by circuit diagrams has. Considerations about limitations of the used approaches, suggestions for improvements and comparisons to other studies will be taken into account. Additionally, an evaluation of the matrix representation and the results of the sensitivity analysis will be discussed at this point.

### 5.1 Measurements

The measured data used for the identification of parameters was superimposed with noise and the progress does not resemble a physical behavior. Therefore, the data had to be filtered and losses in accuracy and reliability were accepted. Although the measuring inaccuracy of the used sensors and devices was not taken into account, it can be shown that some noise are not related to the measurement technique but rather to a mistake in the experimental setup. The signal for the aortic pressure features a noise with a frequency of 20 Hz, which leads back to a possible incorrect connection to a power supply with the same frequency. These mistakes can be avoided by the application of a structured experimental design.

In a preprocessing step the volume flow in the left ventricle had to be computed by deriving the measured signal of the volume in the ventricle. This procedure required calculations which can be avoided by a better planning of the measurement process. For a combination of *HumanLib* components and measured signals, the measurement of flow instead of volume is therefore highly recommended.

For future measurements in order to identify parameters it is highly recommended to improve the "Design of Experiments" in advance. Literature like [5] and [8] suggest a number of methods to design the experiment. Analysis of variances and factorial experiments are common practices to improve the output of measurements and fit it to the desired task. In the course of these

considerations the local sensitivity analysis can help to decide in which operating point a parameter estimation can be carried out. An configuration, in which the parameter has a high local sensitivity, could lead to a large deviation to the real value. On the other hand, the estimation is inapplicable for the locations, where the sensitivity is zero and the chosen parameter has no influence on the system behavior. Therefore, the sensitivity analysis could indicate an optimum for a parameter estimation for a chosen inputs and output signal.

Further calculations like the previous one will lead to a better result for followed investigations. Important factors such as the number of measurements and the sampling rate can easily optimized by using methods to design the setup. Thus, it reduces the experimental efforts if preliminary considerations reveal the limited use or even irrelevance of certain signals for the estimation of parameters.

## 5.2 Equivalent circuit diagrams and the matrix representation

In multiple application it is shown that the components in the *HumanLib* are described with equivalent circuit diagrams and the matrix representations of four-terminal networks. The advantage of the matrix representation is the consistent and compact exposition of the systems behavior. Apart from the presented sensitivity analysis, other investigations such as analyses of stability and robustness can be applied in the derived notation. The design of controller, which are part of heart supporting devices, for example, can be realized by using the mathematical representation of the models.

One problem in the models is the representation of the compliance. This issue is broadly discussed in [12]. The physical compliance in the human body is a nonlinear function of transmural pressure and can be resembled by nonlinear residual-charge capacitor (NRCC). However, the used equations and representations by Ursino use ideal capacitors to describe the behavior. The difference of both approaches is shown in figure 5.1.

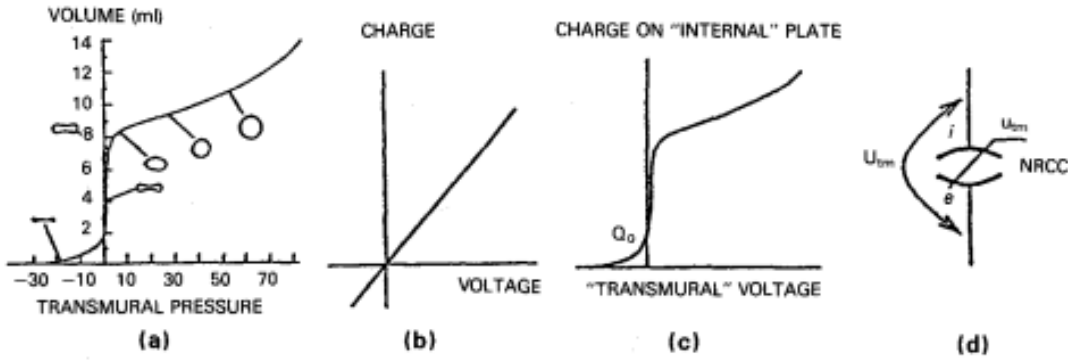


Figure 5.1: (a) Volume and transmural pressure relation (b) ideal electrical capacitor (c) nonlinear residual-charge capacitor (NRCC) (d) sign for NRCC [12]

The physiological relation between volume and transmural pressure in a vessel is shown in 5.2 (a). It shows that the vessel contains a volume for a transmural pressure of zero. The charge of a capacitor, in comparison to that, is zero for no voltage 5.2 (b). Therefore, the used models differ in that point. However, for dynamic considerations, which were done in this thesis, the

charge was not relevant but the current. As the current is the derivation of the charge, the assumptions with ideal capacitors is sufficient in this case. For other calculations the model structure should be considered with NRCC instead of ideal capacitors. Figure 5.2 shows their behavior in (c) and their sign in (d). Another problem is the modeling of ventricles and valves.

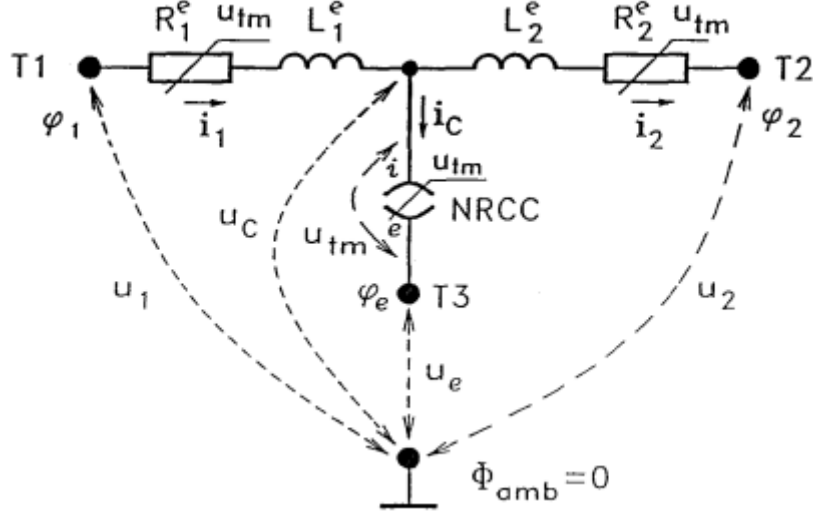


Figure 5.2: The nonlinear residual-charge capacitor as network [12]

There was no matrix notation derived for these components. Both parts consist of nonlinear equations and, therefore, a transformation to matrices is not possible.

Although parts are missing (ventricle and valves) a theoretical consideration about closed loops for the elements will be conducted at this point. A full mathematical representation of the circulatory as a matrix provides a powerful tool to analyze the processes in the *HumanLib*.

The earlier shown models of the aorta and the pulmonary circulation are parts of the whole body. To analyze the behavior of pressure and volume flow, these parts have to be combined and completed with the heart, systemic circulation and venes. The whole body model based on Ursino calculations can be simulated in DYMOLA with the *HumanLib*. The whole body system can be described as a closed loop and a series connection of elements, which are represented by the impedances in figure 5.3.

This circuitry can be opened at any position and regarded as a complex model with inputs and outputs (b). Based on calculations of chapter 3 the model can be described as

$$\begin{pmatrix} U_1 \\ I_1 \end{pmatrix} = \prod A_i \cdot \begin{pmatrix} U_2 \\ -I_2 \end{pmatrix} \quad (5.1)$$

For parallel structures such as the order of  $Z_2$ ,  $Z_3$  and  $Z_4$  the Y matrices are added. The Y matrices for each branch can be determined by using standard tables [15]. After the addition the resulting Y can be transformed to an A matrix, which can included in the calculation with equation 5.1. The An necessary constraint in this context is now that the input and output current are equal derived from the consideration as a closed loop.

$$I_1(t) = I_2(t) \quad (5.2)$$

With these two assumptions the differential equations for complex models can be computed in a very fast and automatic way.

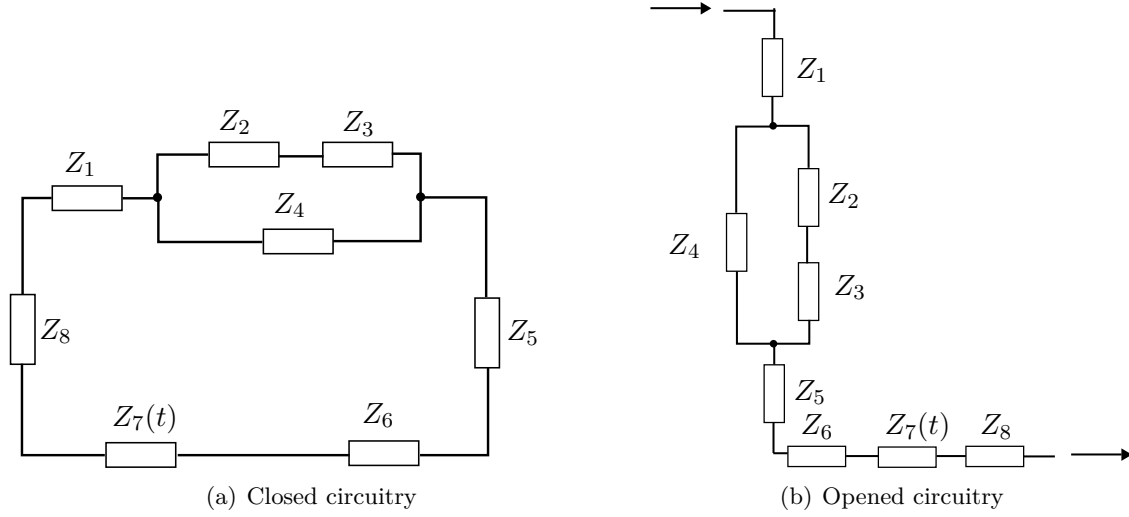


Figure 5.3: Closed and opened circuitry

### Example aorta

This theory will be elaborated on aorta model as example. Connecting input and output of the aorta does not occur in the human body or resemble a physiological system. Nevertheless, the simple structure and the preparatory work with the aorta in earlier chapters of this thesis allow an easy understanding. As the aorta consists of passive elements which do not bring any energy in the system, voltage and current will be equal to zero and the system can be considered to be dead. Therefore, the model has to be extended by an energy source such as a voltage or current source. Another solution is to consider the voltage between input and output as variable. By closing the electrical circuit of the model with the last-mentioned approach looks like shown on figure 5.4. With the assumption of equal currents equation 5.2 the voltage  $U_q$  can be considered as voltage source.

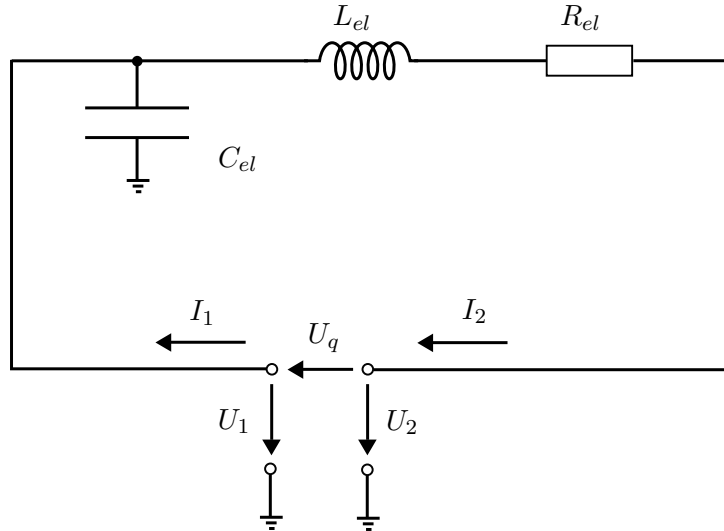


Figure 5.4: Closed circuitry for the aorta model

The matrix product for the aorta is taken from table 3.4.

$$\begin{pmatrix} U_2 \\ I_2 \end{pmatrix} = \begin{pmatrix} 1 & R_{el} + L_{el}s \\ C_{el}s & L_{el}C_{el}s^2 + R_{el}C_{el}s + 1 \end{pmatrix} \cdot \begin{pmatrix} U_1 \\ -I_1 \end{pmatrix} \quad (5.3)$$

With the differential equations which are included in the A matrix in 5.3 a relation of voltage and current is determined. It is

$$U_q(t) = U_2(t) - U_1(t) \quad \circ \longrightarrow \bullet \quad U_q = U_2 - U_1 \quad (5.4)$$

for all functions equal zero as initial condition. As a result, the relation of voltage and current is

$$\frac{U_2 - U_1}{I} = \frac{U_q}{I} = R_{el} + L_{el}s \quad (5.5)$$

The response characteristics between the input  $I$  and the output  $U_q$  is equal to the behavior of a PD element.

In this simple case, the differential equations can be derived easily by applying the Kirchhoff's circuit laws for the highlighted circuitry. The number of parameters and derivatives is clear and conceivable. However, for a series connection with many elements, it becomes difficult to keep the overview and find a solution. Thus, the established approach using the multiplication of matrices provides a good method, which can be supported by computers. For a full body model the introduction of an element for energy sources is necessary. The physiological analogy are the ventricles of the heart. They raise the pressure like a pump and, therefore, can be described as a conductor with variable compliance. However, this approach does not correspond to the nonlinear equations for the ventricles suggested by Ursino.

Further considerations about closed circuitries have to include a time-discrete calculation. This approach will lead to a representation of the object-oriented component library in a mathematical matrix.

### 5.3 *HumanLib* - Chances and limitations

The models based on Ursino are worked on within the previous chapters and a discussion about possible improvements and considerations about further research are introduced at this stage. The used models were given in DYMOLA. A critical problem occurred during the export of the models to SIMULINK. As this seems to be an issue which is related to the functionality of the software, it is highly possible that these problems will not occur in future versions. The developers were informed about the problem in context with the thesis.

In the introducing chapters data flow and object-oriented modeling are presented. During the work with both kind of models, it turned out that the conversion from an object-oriented model to a data flow needs a lot of considerations about the inputs and outputs, which have to be defined before the conversion is performed. The complexity of table 3.4 is one proof how many different results can come up for varying inputs and outputs. These issues do not appear if the model remains object-oriented because inputs and outputs are treated equally, as variables of the differential equation. Therefore, another approach to estimate parameters is to use DYMOLA's functions and algorithms.

For considerations about the model structure, the representation with electric circuits was used. Additionally, matrices were derived and helped to understand the behavior of the models. The predefined assumption was that all elements are passive and do not bring energy in the system. However, this approach needs to be extended with energy sources such as the ventricles in the human cardiovascular system. Other active elements are the valves and the compliance. The external pressure on the compliance was set to zero. This does not resemble the model structure provided by Ursino and can be improved in next considerations.

In contrast to a division of the *HumanLib* components into basic elements and fitting of the simulated output to measured data, better and qualified simulation models are reached by the procedure, shown in figure ???. After signals were measured, the data first has to undergo a Fourier analysis. As a result, the signals are given as a function, which is composed of the sums

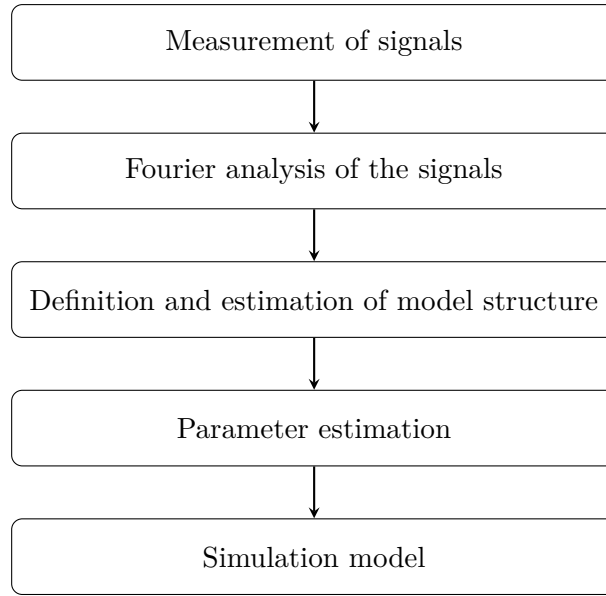


Figure 5.5: Individual procedure from measurement of signals to simulation model

of simpler trigonometric functions. In a next step, the model structure has to be estimated or a desired configuration can be predefined as constraint. As partial models the highlighted elements, resistance, compliance and inertance, can be used and the full model can be composed by them. In a last step the parameters in the model have to be identified.

The *HumanLib* provides an environment for testings of embedded systems such as ventricular assistant devices. Today, model-in-the-loop testings are common ways to profit from the software tool. Furthermore, new model structures and variation in the cardiovascular systems which can be caused by diseases can be computed. However, the quality of prediction differs from reality and needs an enhanced interaction with real process data. In addition to that, many testings are performed and the system knowledge is poor. Although the graphical interfaces in DYMOLA might allow a setting, the underlying system structure does not resemble the actual desired physiological case.

A very cheap and noninvasive way for a test setup for a realization of the predefined goal is to measure the pressures at two points of the body and the volume flow at one of them. For simplicity we choose the pressure at the wrinkle and the upper part of the arm. With these signals and the matrix for both pressures as input (in that case it is matrix  $Y$ ), a parameter estimation is done, comparing the measured and simulated volume flow at the wrinkle. The incoming and outgoing volume flow can now be computed with these considerations.

Theoretically, a parameter estimation can be performed for any parameter in the body in case the model structure is predefined. In the optimal case the measurements are taken from parts which are easy to reach. As an example, the measurements are taken from the wrinkle and heart parameters are estimated. Conclusively, defects can be detected by this procedure. However, this procedure can be hardly realized. Assuming that the system structure for the body in the *HumanLib* features a very high accuracy to the reality, a problem will occur if multiple solutions are possible. This is, for example, the case for parallel structures.

Another limitation for the *HumanLib* components are the restriction that all signals are time depending. Therefore, determination of the position for pressures or volumes are difficult. As the structure for the systemic and pulmonary circulation does not provide any relevant information about the pressure and volume flow in these parts of the body, the research focus for the *HumanLib* should be the heart and its behavior. Consequently, the pulmonary and



systemic circulations can be modeled without respect to its actual physiological appearance. For the measurement points this means that the best locations are just after blood left the heart and before it enters it. For the design of experiment these facts should be considered for further investigations.

## 5.4 Results of parameter estimation

It has been proved that the models in the *HumanLib*, can be used for parameter estimations in combination with measured data. The validation of the estimation with measured and simulated data has been neglected because the accuracy of the signals were regarded as improvable for future investigations. However, a comparison of standard values according to Ursino and the results of the estimation is shown in table 5.3.

As expected the estimated parameters deviate in their value from the literature value. While

Parameters	Ursino's value	Results	Absolute error	Relative error
L [ $\frac{mmHg \cdot ml}{sec^2}$ ]	$22 \cdot 10^{-5}$	$16.2 \cdot 10^{-3}$	$15.98 \cdot 10^{-3}$	7263%
C [ $\frac{ml}{mmHg}$ ]	0.28	0.11	-0.17	-61%
R [ $\frac{mmHg \cdot sec}{ml}$ ]	0.06	$5.4 \cdot 10^{-5}$	$-59.9 \cdot 10^{-3}$	-99.91%

Table 5.1: Results for the aortic parameter estimation

the error for the inductance is extremely high with 7263%, the value for the compliance is relatively and absolutely closer to Ursino's value. The result for the resistance, similar to the inductance, is far away from the expected value.

The poor quality of the results can be lead back to the mentioned inaccuracy of the measurement. In addition to that, the number of data for the estimation with approximately 100 data points and 0.04 seconds of record is extremely small. For a very accurate estimation of the aorta, the focus of the measurement should be a precise signal detection of pressures and volume flow in a time range when the aortic valve opens and until it closes again. The sensors should be positioned right after the aortic valve and in the aortic arch to get a good estimation for the parameters of the ascending aorta. The analysis of configurations for inputs and outputs showed that three signals of pressure and volume flow are enough for a complete estimation of all involving parameters.

## 5.5 Results of sensitivity analysis

A sensitivity analysis for the aorta and pulmonary circulation model was exemplarily carried out with assumed inputs. For approximating the sensitivities the method of internal differentiation was emphasized to find out how sensitive parameters are in a defined local area. As a result, the dimension of influence for estimations of parameter was found. In addition to that, the locations where the chosen parameter have no influence on the system can be identified by the presented methods. The results for the sensitivity analysis are given in table 5.2 and 5.3. For each parameter the absolute sensitivity minimum was computed. With this value the influences are comparable. The percentage, highlighted in the table, is calculated by the sensitivity divided

<b>Aorta model</b>		
Parameter $p$	Absolute sensitivity minimum $ \min(\frac{\Delta i_2(t)}{\Delta p}) $	Percentage
$C_{el}$	$3.60 \cdot 10^{-5}$	18.73%
$L_{el}$	$1.87 \cdot 10^{-7}$	0.1%
$R_{el}$	$3.60 \cdot 10^{-5}$	18.73%
$U_e$	$1.2 \cdot 10^{-4}$	62.44%

Table 5.2: Results for the aortic parameter estimation

<b>Pulmonary circulation model</b>		
Parameter $p$	Absolute sensitivity minimum $ \min(\frac{\Delta i_2(t)}{\Delta p}) $	Percentage
$L_{el,1}$	$1.01 \cdot 10^{-4}$	0.07%
$R_{el,1}$	0.026	16.76%
$C_{el,2}$	0.009	5.8%
$R_{el,2}$	0.075	48.36%
$C_{el,3}$	0.01	6.45%
$R_{el,3}$	0.014	9.03%
$U_e$	0.021	13.54%

Table 5.3: Results for the pulmonary parameter estimation

by the sum of all sensitivities. For the compliance  $C_{el}$ , for example, it is

$$\frac{|\min(\frac{\Delta i_2(t)}{\Delta C_{el}})|}{\sum |\min(\frac{\Delta i_2(t)}{\Delta p})|} = \frac{3.60 \cdot 10^{-5}}{1.87 \cdot 10^{-7} + 3.60 \cdot 10^{-5} + 1.2 \cdot 10^{-4}} = 18.73\% \quad (5.6)$$

One can see that the influence of the voltage  $U_e$  is the most significant for the aorta. For a good quality in terms of a parameter estimation, a sensitivity analysis should always be part of the preprocessing steps. If four signals are given and the system structure is predefined, the fast sensitivity analysis with matrices, presented in chapter 4.2.1, for each configuration leads to a quantitative overview of which parameters can be estimated with the data. This provides the possibility to evaluate the operating point, which is defined by the input data. However, the shown methods consider the local area of the parameter. Applying the method on the full domain of the parameter leads to long computations and processing. Additionally, the quantitative statements by the local sensitivity analysis requires an determination of all parameters. This knowledge often does not exist in advance. A global sensitivity analysis completes the investigations about the parameters' influence. As an example, variance-based are common forms of global sensitivity analyses. In this method the output of the model is decomposed into fractions, which can be attributed to the inputs. For example, for a model with one output and two inputs, the output could be influenced 10% by the first input, 50% by the second and 40% by an interaction of both. These percentages provide directly information about the sensitivities of the inputs. In [5] the described method can be found in chapter 10, called "Sobol's Kennzahl".

Modeling of dynamic systems often results in a complex system with high orders. For simulation, this means that the computational effort is high. System reduction can be important in that case. The sensitivity analysis helps to identify non-relevant parameters and the order can be reduced. The reduction task, however, needs to find a compromise between model accuracy and

numerical effort.

The computations in this thesis include scenarios with estimated signals for the inputs. A verification with real data and experiments is needed.



---

## Conclusion

---

The approaches presented in this thesis enable an integration of measured data into the cardiovascular models, which are provided by the component library *HumanLib*. A parameter estimation was performed to achieve this goal. However, the error between simulated and measured data is high and a better quality of measurements is required. A theoretical experiment by using the local sensitivity analysis showed that some parameters such as the external pressure on the vessels do not have a significant influence on the model output. However, a global sensitivity analysis needs to be carried out to approve the parameter's significance in its full domain of definition. Especially, the variance-based sensitivity analysis by Sobol promises good results for investigations on the given models. Further possibility to improve the quality for the model outputs and the application for interactions between model and reality were broadly discussed. However, the usability for clinical relevance has to be proved in further studies. Especially, pathological appearances have been unconsidered in earlier works with computer models. Complex diseases such as cardiac anomalies have to be the focus for further investigations. A model of anomalies, which is able to be simulated, is extremely useful for surgical intervention and can help to identify necessary treatments. Moreover, with the considerations about noninvasive measurements, precise diagnoses might be made by simple blood pressure readings.

Referring to future projects in terms of pathology, the modeling of heart defects is needed for clinical practices. A common cardiac anomaly is the "Double Inlet Left Ventricle" or "Single Ventricle". This defect is congenital and expresses itself by a single heart chamber which pumps blood into the pulmonary and systemic circulation. The types of univentricular hearts are diverse and complex in their appearance. The treatment requires a fast surgical intervention in a very early stage after the diagnosis. As palliative treatment, "Fontan's operation" can improve the patient's situation by separating the pulmonary and the systemic circulation. A very new cardiovascular system is the result of the procedure. The modeling and computation in this thesis could offer a strategy for an improvement of the surgery and interventions by simulation of the heart defects and the continuously changing situation of the patient. Online monitoring with sensors after the treatments could lead to a better lifestyle and a fast detection of possible misbehavior. In terms of "Smart Life Support", this approach leads to the desired combination of monitoring, computer simulation and medical device for intervention.

In current works and theses, the *HumanLib* is used as environment for the design of controllers, e.g. for ventricle assistant devices (VAD). As the estimation procedure in chapter 2 and the related discussion show, the combination of elements in the *HumanLib* and their configurations can lead to complex structures with unclear behavior. Therefore, the use of Dymola as application design tool has to be considered with caution. Simple structures, which seem to be logical in their graphical representation can lead to fatal errors. A closer inspection of the underlying equations is highly recommended and the matrix representation offers an easy handling in that case.

---

# Bibliography

---

- [1] Dirk Abel Alexander Bollig. *Rapid Control Prototyping*. Springer, 1. edition, 2006.
- [2] Anja Brunberg. *Modellierung des Herz-Kreislauf-Systems und physiologischer Regelkreise als objektorientierte Komponentenbibliothek*. PhD thesis, RWTH Aachen University, 2012.
- [3] Dr. Manfred Heckmann Dr.h.c. Robert F Schmidt Ph.D, Dr. Florian Lang. *Physiologie des Menschen*. Springer, 29. edition, 2005.
- [4] Peter Elter. *Methoden und Systeme zur nichtinvasiven, kontinuierlichen und belastungs-freien Blutdruckmessung*. PhD thesis, Universität Karlsruhe, 2001.
- [5] Thomas Hochkirchen Karl Siebertz, David van Bebber. *Statistische Versuchsplanung*, volume 1. Springer, 2010.
- [6] Richard E. Klabunde. *Cardiovascular Physiology Concepts*. Lippincott Williams & Wilkins, 2. edition, 2012.
- [7] Puska P. Norrving B. Mendis, S. *Global Atlas on Cardiovascular Disease Prevention and Control*, volume 1. World Health Organization, 2011.
- [8] Douglas C. Montgomery. *Design and Analysis of Experiments*, volume 8. John Wiley & Sons, 2013.
- [9] Ivan A. Nestorov. Sensitivity analysis of pharmacokinetic and pharmacodynamic systems: I. a structural approach to sensitivity analysis of physiologically based pharmacokinetic models. *Journal of Pharmacokinetics and Biopharmaceutics*, 27:578, 1999.
- [10] Alexander Ostermann. Sensitivity analysis. [www.mat1.uibk.ac.at/mathematik/publ](http://www.mat1.uibk.ac.at/mathematik/publ), 03 2004.
- [11] Dietrich Wolf Reinhard Lerch, Gerhard M. Sessler. *Technische Akustik: Grundlagen und Anwendungen*. Springer, 2009.
- [12] Joshua E. Tsitlik. Modeling the circulation with three-terminal electrical networks containing special nonlinear capacitors. *Annals of Biomedical Engineering*, 20:595–616, 1992.
- [13] Mauro Ursino. Interaction between carotid baroregulation and the pulsating heart: a mathematical model. *AJP - Heart and Circulatory Physiology*, 275:1733–1747, 1998.
- [14] Holger Watten. *Hydraulik und Pneumatik*. Vieweg + Teubner, 2. edition, 2008.
- [15] Wilfried Weißgerber. *Elektrotechnik für Ingenieure 3: Ausgleichsvorgänge, Fourieranalyse, Vierpoltheorie. Ein Lehr- und Arbeitsbuch für das Grundstudium*. Springer, 2009.